Optimal Sliding and Decoupled Sliding Mode Tracking Control by Multi-objective Particle Swarm Optimization and Genetic Algorithms

M. Taherkhorsandi, K.K. Castillo-Villar, M.J. Mahmoodabadi, F. Janaghaei and S.M. Mortazavi Yazdi

Abstract The objective of this chapter is to present an optimal robust control approach based upon smart multi-objective optimization algorithms for systems with challenging dynamic equations in order to minimize the control inputs and tracking and position error. To this end, an optimal sliding and decoupled sliding mode control technique based on three multi-objective optimization algorithms, that is, multi-objective periodic CDPSO, modified NSGAII and Sigma method is presented to control two dynamic systems including biped robots and ball and beam systems. The control of biped robots is one of the most challenging topics in the field of robotics because the stability of the biped robots is usually provided laboriously regarding the heavily nonlinear dynamic equations of them. On the other hand, the ball and beam system is one of the most popular laboratory models used widely to challenge the control techniques. Sliding mode control (SMC) is a nonlinear controller with characteristics of robustness and invariance to model parametric uncertainties and nonlinearity in the dynamic equations. Hence, optimal sliding mode tracking control tuned by multi-objective optimization algorithms is utilized in this study to present a controller having exclusive qualities, such as robust performance and optimal control inputs. To design an optimal control approach, multi-objective particle swarm optimization (PSO) called multi-objective periodic CDPSO introduced by authors in their previous research and two notable smart multi-objective optimization algorithms, i.e. modified NSGAII and the Sigma method are employed to ascertain the optimal parameters of the control approach with regard to the design criteria. In comparison, genetic algorithm optimization operates based upon reproduction, crossover and mutation; however particle swarm optimization functions by means of

M. Taherkhorsandi (✉) · K.K. Castillo-Villar
Department of Mechanical Engineering, The University of Texas at San Antonio, San Antonio, TX 78249, USA
e-mail: m.taherkhorsandi@gmail.com; milad.taherkhorsandi@utsa.edu

M.J. Mahmoodabadi · F. Janaghaei · S.M. Mortazavi Yazdi
Department of Mechanical Engineering, Sirjan University of Technology, Sirjan, Iran
e-mail: mahmoodabadi@sirjantech.ac.ir

A.T. Azar and Q. Zhu (eds.), *Advances and Applications in Sliding Mode Control systems*, Studies in Computational Intelligence 576, DOI 10.1007/978-3-319-11173-5_2

a convergence and divergence operator, a periodic leader selection method, and an adaptive elimination technique. When the multi-objective optimization algorithms are applied to the design of the controller, there is a trade-off between the tracking error and control inputs. By means of optimal points of the Pareto front obtained from the multi-objective optimization algorithms, plenty of opportunity is provided to engineers to design the control approach. Contrasting the Pareto front obtained by multi-objective periodic CDPSO with two noteworthy multi-objective optimization algorithms i.e. modified NSGAII and Sigma method dramatizes the excellent performance of multi-objective periodic CDPSO in the design of the control method. Finally, the optimal sliding mode tracking control tuned by CDPSO is applied to the control of a biped robot walking in the lateral plane on slope and the ball and beam system. The results and analysis prove the efficiency of the control approach with regard to providing optimal control inputs and low tracking and position errors.

1 Introduction

Two-legged robots named biped robots are the most similar kind of robots to human. As a unique advantage of this robot in comparison to other robots, they can be used in any situation where working of a human is unsafe or hazardous (Cha et al. 2011; Dehghani et al. 2013; Ding et al. 2013; Feng et al. 2013; Lee et al. 2014). One important challenging characteristic of this robot is having the dynamic equations which are nonlinear and demanding to control. To this end, it is crucial to employ a nonlinear controller which is robust with regard to disturbances and uncertainty in order to provide stable walking for biped robots (Andalib Sahnehsaraei et al. 2013). In this regard, sliding mode control is an effectual control method in terms of providing low tracking error in contrast to PID control (Lu et al. 2011) and linear feedback control (Basin et al. 2012). Owing to its exclusive benefits, a number of researchers have applied it to a variety of problems with challenging dynamic equations and successful application of it has been reported. For instance, Nizar et al. applied the sliding mode controllers for the time delay systems (Nizar et al. 2013). Han et al. proposed the sliding mode control of T-S fuzzy descriptor systems with time-delay (Han et al. 2012). Yakut applied an intelligent sliding mode controller with moving sliding surface for overhead cranes (Yakut 2014). Eker utilized the second-order sliding mode controller with PI sliding surface for an electromechanical plant (Eker 2012). Sira-Ramirez et al. proposed a robust input-output sliding mode control for the buck converter (Sira-Ramirez et al. 2013). Bayramoglu and Komurcugil used time-varying sliding-coefficient-based terminal sliding mode control methods for a class of fourth-order nonlinear systems (Bayramoglu and Komurcugil 2013). Li et al. proposed a sliding mode controller for uncertain chaotic systems with input nonlinearity (Li et al. 2012). Yin et al. designed a sliding mode controller for a class of fractional-order chaotic systems (Yin et al. 2012). Zhang et al. applied the second-order terminal sliding mode controller for a hypersonic vehicle in cruising flight with sliding mode disturbance observer (Zhang et al. 2013). Moreover, it is reliable

and efficient when it is applied for the control of robots (Hu et al. 2012; Sun et al. 2011). In illustration, Nikkhah et al. utilized a robust sliding mode tracking control algorithm for a biped robot modeled as a five-link planar robot with four actuators following a human-like gait trajectory in the sagittal plane (Nikkhah et al. 2007). Lin et al. proposed a hybrid control approach based upon the sliding mode method and a recurrent cerebellar model articulation controller to control biped robots (Lin et al. 2007). Moreover, the Taylor linearization approach was used to enhance the learning ability of the recurrent cerebellar model articulation controller. Since chattering is a crucial unresolved issue in designing sliding mode controllers, some researchers have tried to reduce the amount of chattering in actuators (Mondal and Mahanta 2013a; Pourmahmood Aghababa and Akbari 2012; Ramos et al. 2013; Cerman and Husek 2012; Lin et al. 2011; Singla et al. 2014). In particular, Shahriari kahkeshi et al. constructed smooth sliding mode control for a class of high-order nonlinear systems having no prior knowledge about uncertainty (Shahriari kahkeshi et al. 2013). They could eliminate the chattering problem completely via proposing a scheme which involves an adaptive fuzzy wavelet neural controller to construct equivalent control term and an adaptive proportional-integral (A-PI) controller for applying switching term to deliver smooth control input. Adhikary and Mahanta proposed an integral backstepping sliding mode control approach to control underactuated systems (Adhikary and Mahanta 2013). Rejecting matched and mismatched uncertainties, providing a chattering free control law, and using less control effort than the sliding mode controller were reported as the most important advantages of the proposed controller. Liu used Lie-group differential algebraic equation method to design a sliding mode controller through adding a compensated control force which resulted in steering rapidly and enforcing continuously the state trajectory on the sliding surface (Liu 2014). The proposed control methodology is chattering-free for a class of regulator problems and finite-time tracking problems of nonlinear systems. Mondal and Mahanta used the derivative of the control input in the proposed control law to design an adaptive integral higher order sliding mode controller for uncertain systems (Mondal and Mahanta 2013b). The actual control signal gained through integrating the derivative control signal is chattering free and smooth.

Designing the parameters of control approaches is an interesting and challenging issue in industry and academia. Multi-objective optimization algorithms are appropriate approaches to gain these parameters via considering both tracking error and control effort. In particular, the genetic algorithm and particle swarm optimization are two notable effectual optimization algorithms to gain optimal solutions (Castillo-Villar et al. 2012, 2014; Martínez-Soto et al. 2013; Elshazly et al. 2013; Aziz et al. 2013). In the literature, particle swarm optimization has been successfully used to augment the performance of type-1 and type-2 fuzzy control (Martínez-Soto et al. 2013), fractional fuzzy control (Pan et al. 2012), PID control (Jadhav and Vadirajacharya 2012), constrained multivariable predictive controllers (Júnior 2014), and other controllers (Lari et al. 2014). PSO, first introduced by Kennedy and Eberhart, is one of the modern smart heuristic algorithms (Kennedy and Eberhart 1995). It is a robust optimization algorithm developed via simulation of simplified social systems to solve nonlinear optimization problems (Angeline 1998). Successful applications of this

robust optimization algorithm have been reported not only in the area of control theory but also in a wide variety field of research. For instance, in Wang and Jun Zheng (2012), a new particle swarm optimization algorithm was applied to optimum design of the armored vehicle scheme. In Yildiz and Solanki (2012), multi-objective optimization of vehicle crashworthiness was performed using a new particle swarm based approach. In Kim and Son (2012), a probability matrix based particle swarm optimization was applied for the capacitated vehicle routing problem. In Belmecheri et al. (2013), the particle swarm optimization algorithm was used for a vehicle routing problem with heterogeneous fleet, mixed backhauls, and time windows. In Nejat et al. (2014), the optimization of the airfoil shape was performed using the improved multi-objective territorial particle swarm algorithm with the objective of improving stall characteristics. In Hart and Vlahopoulos (2010), an integrated multidisciplinary particle swarm optimization approach was introduced for conceptual design of ships. In Aparecida de Pina et al. (2011), the particle swarm optimization algorithm was applied to the design of steel catenary risers in a lazy-wave configuration. In Nwankwor et al. (2013), hybrid differential evolution and particle swarm optimization were utilized for optimal well placement. In Zhang et al. (2013), the sequential quadratic programming particle swarm optimization was applied for wind power system operations considering emissions. In Zheng and Wu (2012), Power optimization of gas pipelines was performed with aid of an improved particle swarm optimization algorithm. In Biswas et al. (2013), constriction factor based particle swarm optimization was introduced for analyzing tuned reactive power dispatch. Short calculation time and more stable convergence are two important characteristics of the PSO technique (Eberhart and Shi 1998; Yoshida et al. 2000). Depending on the case study, PSO can show better performance than genetic algorithm optimization (Lin and Lin 2012). Appropriate performance of PSO in combination with genetic algorithm optimization has been reported in the literature as a hybrid optimization algorithm (Mousa et al. 2012; Kuo et al. 2012). Furthermore, PSO is an effectual algorithm to solve multi-objective problems (Carvalho and Pozo 2012). The techniques, a self-adaptive diversity control strategy (Wang and Tang 2012), chaotic local search (Jia et al. 2011), and migration of some particles from one complex to another have been employed to prevent from premature convergence of PSO (Gang et al. 2012). Lately, several methods have been proposed to develop the PSO algorithm to deal with multi-objective optimization problems. To this end, dynamic neighborhood PSO (Hu and Eberhart 2002), dominated tree (Fieldsend and Singh 2002), Sigma method (Mostaghim and Teich 2003), vector evaluated PSO (Parsopoulos et al. 2004), etc. were introduced to solve the multi-objective optimization problems. The principal difference among these methods is the leader selection technique.

In the present chapter, multi-objective periodic CDPSO introduced in authors' previous works (Mahmoodabadi et al. 2011, 2012a) and two prominent smart evolutionary algorithms (Mostaghim and Teich 2003; Atashkari et al. 2007) are used to eliminate the tedious trial-and-error process and design the optimal nonlinear sliding mode tracking control. This controller is applied to a biped robot modeled and walking in the lateral plane on slope (Mahmoodabadi et al. 2014a, b). The outline of the rest of this chapter is as follows: Sect. 2 discusses the multi-objective particle swarm

optimization including the convergence and divergence operators, the periodic leader selection approach, and the adaptive elimination technique. Section 3 involves the control approach where Canonical and Non-canonical forms of both sliding mode control and decoupled sliding mode control are discussed. The dynamic model of the biped robot and the Pareto design of sliding mode control of the biped robot based on multi-objective periodic CDPSO, modified NSGAII and sigma method are presented in Sect. 4. Section 5 includes the dynamic model of the Ball and Beam system and the Pareto design of decoupled sliding mode control for the Ball and Beam system using multi-objective periodic CDPSO, modified NSGAII and sigma method. Section 6 presents the conclusions of this study.

2 Multi-objective Particle Swarm Optimization

In this chapter, multi-objective periodic CDPSO is used to address the problem of the proper selection of parameters of sliding mode control. Indeed, this optimization method was successfully employed to acquire the Pareto frontiers of non-commensurable objective functions in the design of linear state feedback controllers (Mahmoodabadi et al. 2011) and the suspension system for a vehicle vibration model (Mahmoodabadi et al. 2012b). This method is a combination of the particle swarm optimization, convergence and divergence operators. Moreover, a new leader selection method is applied to produce a set of Pareto optimal solutions which has good diversity and distribution. The archive is pruned in this algorithm by implementing an adaptive elimination technique. The algorithm was named multi-objective periodic CDPSO. PSO, convergence divergence operator, periodic leader selection method and adaptive elimination technique are described concisely, as follows:

2.1 Particle Swarm Optimization

PSO is a population-based evolutionary algorithm and is inspired by the simulation of social behavior (Kennedy and Eberhart 1995). Although PSO had been initially employed to balance weights in neural networks (Eberhart et al. 1996), it became a very popular global optimizer, mostly in the problems where the decision variables were real numbers (Engelbrecht 2002, 2005). Each candidate solution in PSO is associated with a velocity (Kennedy and Eberhart 1995; Ratnaweera and Halgamuge 2004), and it is assumed that the particles will move toward better solution areas. Mathematically, the particles are functioning based upon the following equations.

$$\vec{x}_i(t+1) = \vec{x}_i(t) + \vec{v}_i(t+1) \tag{1}$$

$$\vec{v}_i(t+1) = W\vec{v}_i(t) + C_1 r_1(\vec{x}_{pbest_i} - \vec{x}_i(t)) + C_2 r_2(\vec{x}_{gbest} - \vec{x}_i(t)) \tag{2}$$

In which, $\vec{x}_i(t)$ and $\vec{v}_i(t)$ stand for the position and velocity of particle i at the time step (iteration) t. $r_1, r_2 \in [0, 1]$ denote random values. C_1 stands for the cognitive learning feature and represents the attraction that a particle has toward its own success. C_2stands for the social learning feature and represents the attraction that a particle has toward the success of the entire swarm. It was obtained that the best solutions were gained when C_1 is linearly decreased and C_2 is linearly increased over the iterations (Ratnaweera and Halgamuge 2004). W stands for the inertia weight and controls the impact of the previous history of velocities on the current velocity of particle i. Based on experimental results, PSO functioning improves when the inertia weight diminishes linearly over iterations (Kennedy and Eberhart 1995). Moreover, $\vec{x}_{pbest_i}$ is the personal best position of the particle i and $\vec{x}_{gbest}$ represents the position of the best particle of the whole swarm.

2.2 The Convergence Operator

In the present chapter, the convergence formula, which contains four parent particles proposed in Mahmoodabadi et al. (2011, 2012a) is employed. Let $\rho \in [0, 1]$ be a random number. If $\rho \leq P_{Convergence}$ ($P_{Convergence}$ is convergence probability), then one of the following operators should be operated to generate the new particle position $\vec{x}_i\ (t + 1)$ from the old particle position $\vec{x}_i(t)$:

If fitness $\vec{x}_i(t)$ is smaller than fitness $\vec{x}_j\ (t)$ and fitness $\vec{x}_k(t)$ then:

$$\vec{x}_i\ (t + 1) = \vec{x}_{gbest} + \sigma_1 \left(\frac{\vec{x}_{gbest}}{\vec{x}_i(t)} \right) (2\vec{x}_i(t) - \vec{x}_j(t) - \vec{x}_k(t)) \tag{3}$$

If fitness $\vec{x}_j(t)$ is smaller than fitness $\vec{x}_i\ (t)$ and fitness $\vec{x}_k(t)$ then:

$$\vec{x}_i\ (t + 1) = \vec{x}_{gbest} + \sigma_2 \left(\frac{\vec{x}_{gbest}}{\vec{x}_i(t)} \right) (2\vec{x}_j(t) - \vec{x}_i(t) - \vec{x}_k(t)) \tag{4}$$

If fitness $\vec{x}_k(t)$ is smaller than fitness $\vec{x}_j\ (t)$ and fitness $\vec{x}_i(t)$ then:

$$\vec{x}_i\ (t + 1) = \vec{x}_{gbest} + \sigma_3 \left(\frac{\vec{x}_{gbest}}{\vec{x}_i(t)} \right) (2\vec{x}_k(t) - \vec{x}_j(t) - \vec{x}_i(t)) \tag{5}$$

In which, particles $\vec{x}_j(t)$ and $\vec{x}_k(t)$ are chosen from swarm by a uniform selection approach. σ_1, σ_2, and σ_3 are arbitrary numbers chosen from [0, 1] and $\vec{x}_{gbest}$ stands for the position of the best particle of the entire swarm. After calculating Eqs. (3), (4) or (5), the superior one between $\vec{x}_i(t)$ and $\vec{x}_i(t+1)$ should be selected. If $\rho \geq P_{Convergence}$, then no convergence operation is operated for $\vec{x}_i\ (t)$.

2.3 The Divergence Operator

The divergence operator provides a feasible leap on some selected particles. Let $\vartheta \in [0, 1]$ be an arbitrary number. If $\vartheta \leq P_{Divergence}$, ($P_{Divergence}$ is divergence probability) and particle $\vec{x}_i$ (t) was not improved by the convergence operator, the following divergence operator is operated to create a new particle.

$$\vec{x}_i\,(t+1) = \text{Norm rand}(\vec{x}_i\,(t), S_D) \tag{6}$$

Norm rand($\vec{x}_i$ (t) , S_D) creates arbitrary numbers from the normal distribution with mean parameter $\vec{x}_i$ (t) and standard deviation parameter S_D (S_D is a positive constant). If particle $\vec{x}_i$ (t) was augmented by convergence operator or $\vartheta \geq P_{Divergence}$, then no divergence operation is operated. More features of this operator are discussed in Mahmoodabadi et al. (2011, 2012a).

2.4 The Periodic Leader Selection Approach

This methodology is based on the density measures. A neighborhood radius $R_{neighborhood}$ is defined for leaders and if their Euclidean distance (measured in the objective domain) is less than $R_{neighborhood}$, two leaders are neighbors. In this respect, the number of neighbors of each leader is computed in the objective function area. The particle with fewer neighbors is preferred as the leader; even though, the leader position and its density will change after several iterations. Hence, the leader selection operation should be repeated and a new leader must be ascertained. Thus, the maximum iteration is divided into several equal periods and each period has the same iteration T. The relation among maximum iteration, number of periods and T satisfies Eq. (7):

$$\text{maximum iteration} = \text{number of periods} \times T \tag{7}$$

In each period, the leader selection operation could be performed, and the non-dominated solution which has fewer neighbors is preferred as the leader. Moreover, if a particle dominates the leader in the start of the iteration in a period, then this particle will be regarded as a new leader.

2.5 The Adaptive Elimination Technique

This approach is employed to prune the archive; and in this approach, the archive's members have an elimination radius which equals $\varepsilon_{elimination}$. If the Euclidean distance (in the objective function space) between two particles is less than $\varepsilon_{elimination}$,

then one of them will be omitted. The following equation is used to determine the value of $\varepsilon_{\text{elimination}}$ named adaptive $\varepsilon_{\text{elimination}}$:

$$\varepsilon_{\text{elimination}} = \frac{\text{t}}{\zeta \times \text{maximum iteration}} \tag{8}$$

In which, ζ is a positive constant, t is the current iteration number, and maximum iteration presents the maximum number of permissible iterations (Mahmoodabadi et al. 2011, 2012a).

3 The Control Approach

Sliding Mode Control (SMC) is an effective control methodology for nonlinear systems. One of the main advantages of SMC is that the uncertainties and external disturbances of the system can be handled under the invariance characteristics of sliding conditions. Nevertheless, the SMC technique can be applied only to the systems with the canonical form. In this respect, the basic idea of Decoupled Sliding Mode Control (DSMC) is proposed to design a controller for systems with the non-canonical form. However, for the optimum design of DSMC, it is difficult to determine the parameters of the sliding surface. This problem could be solved by using the evolutionary optimization techniques. Fleming and Purshouse (2002) is an appropriate reference to overview the application of the evolutionary algorithms in the field of the design of controllers. In particular, the design of controllers in Fonseca and Fleming (1994) and Sanchez et al. (2007) was formulated as a multi-objective optimization problem and solved using Genetic Algorithms (GAs). Furthermore, in Javadi-Moghaddam and Bagheri (2010), the GA was utilized to select the parameters of SMC for an underwater remotely operated vehicle. In Ker-Wei and Shang-Chang (2006), the sliding mode control configurations were designed for an alternating current servo motor while a Particle Swarm Optimization (PSO) algorithm was used to select the parameters of the controller. Also, PSO was applied to tune the linear control gains in Gaing (2004); Qiao et al. (2006). These works have shown that PSO is a fast and reliable tool to design the optimal controllers, and also can outperform other evolutionary algorithms. In Chen et al. (2009), three parameters associated with the control law of the sliding mode controller for the inverted pendulum system were properly chosen by a modified PSO algorithm. Wai et al. proposed a total sliding-model-based particle swarm optimization approach to design a controller for the linear induction motor (Wai et al. 2007). More recently, in Gosh et al. (2011), an ecologically inspired direct search method was applied to solve the optimal control problems with Bezier parameterization. Moreover, in Tang et al. (2011), a controllable probabilistic particle swarm optimization (CPPSO) algorithm was applied to design a memoryless feedback controller.

3.1 Canonical and Non-canonical Forms

Consider a forth-order nonlinear system, which could be represented by the following canonical form.

$$\begin{aligned} \dot{x}_1 &= x_3 \\ \dot{x}_2 &= x_4 \\ \dot{x}_3 &= f_1(x) + b_1(x)\, u_1 \\ \dot{x}_4 &= f_2(x) + b_2(x)\, u_2 \end{aligned} \tag{9}$$

where $x = \left[x_1\ x_2\ x_3\ x_4 \right]^T$ is the state vector, $f_1(x)$, $f_2(x)$, $b_1(x)$, and $b_2(x)$ are nonlinear functions. u_1 and u_2 are control inputs.

This type of forth-order systems with the canonical form could be controlled by using many kinds of techniques, such as fuzzy control, proportional–integral–derivative (PID) control, sliding mode control, etc. In fact, the control laws u_1 and u_2 can be easily designed to control the system introduced by Eq. (9). However, for some nonlinear models such as the ball and beam system, the system dynamic equations are not in the canonical form. The state space model of a system with the non-canonical form is presented, as follows.

$$\begin{aligned} \dot{x}_1 &= x_3 \\ \dot{x}_2 &= x_4 \\ \dot{x}_3 &= f_1(x) + b_1(x)\, u \\ \dot{x}_4 &= f_2(x) + b_2(x)\, u \end{aligned} \tag{10}$$

where $x = \left[x_1\ x_2\ x_3\ x_4 \right]^T$ stands for the state vector, $f_1(x)$, $f_2(x)$, $b_1(x)$, and $b_2(x)$ are nonlinear functions. u is a control input. The control techniques mentioned above could control only one of the subsystems in Eq. (10). In other words, these methodologies cannot simultaneously control both subsystems by only one control input u. Hence, the idea of decoupling is employed to design a control law u to control the whole system. In the following sections, the general concepts of the sliding mode control and decoupled sliding mode control are briefly presented.

3.2 Sliding Mode Control for Canonical Forms

The basic concepts of sliding mode control are presented in Wang and Jun Zheng (2012). By regarding the dynamical system introduced according Eq. (9) and having desired trajectories $x_{1d}(t)$ and $x_{2d}(t)$, the errors are defined as $e_1(t) = x_1(t) - x_{1d}(t)$ and $e_2(t) = x_2(t) - x_{2d}(t)$. After a reaching phase, the sliding mode controller forces the system to track the following sliding surfaces.

$$s_1(x) = \dot{e}_2 + \lambda_1 e_1 = x_3 - x_{3d} + \lambda_1 (x_1 - x_{1d}) = 0$$
$$s_2(x) = \dot{e}_2 + \lambda_2 e_2 = x_4 - x_{4d} + \lambda_2 (x_2 - x_{2d}) = 0 \tag{11}$$

where $x_{3d}(t) = \dot{x}_{1d}(t), x_{4d}(t) = \dot{x}_{2d}(t)$, and sliding constants λ_1 and λ_2 are strictly positive. In the steady state conditions, the system follows the desired trajectories when $S_1(x(t_{1reach})) = 0$ and $S_2(x(t_{2reach})) = 0$. t_{1reach} and t_{2reach} represent reaching times. Hence, suitable control actions based on sliding surfaces introduced by Eq. (11) would be achieved. Lyapunov functions could be chosen as Eq. (12).

$$V_1 = \tfrac{1}{2} S_1^2(x)$$
$$V_2 = \tfrac{1}{2} S_2^2(x) \tag{12}$$

with the following controller actions:

$$u_1 = \hat{u}_1 - K_1 \, sign \, (S_1(x) b_1(x)) \text{ and } K_1 > 0$$
$$u_2 = \hat{u}_2 - K_2 \, sign \, (S_2(x) b_2(x)) \text{ and } K_2 > 0 \tag{13}$$

where K_1 and K_2 are the design parameters or functions of $x(t)$ such that $K_1 = K_1(x)$ and $K_2 = K_2(x)$. $sign$represents sign function. $\hat{u}_1$ and $\hat{u}_2$ would be obtained using Eq. (14).

$$\hat{u}_1 = -b_1^{-1}(x) (f_1(x) - \ddot{x}_{1d} + \lambda_1 \dot{e}_1)$$
$$\hat{u}_2 = -b_2^{-1}(x) (f_2(x) - \ddot{x}_{2d} + \lambda_2 \dot{e}_2) \tag{14}$$

Derivations of Lyapunov functions introduced via Eq. (12) are written in the following forms:

$$\dot{V}_1 \leq -\eta_1 |S_1(x)|$$
$$\dot{V}_2 \leq -\eta_2 |S_2(x)| \tag{15}$$

where $K_1 > \eta_1$ and $K_2 > \eta_2$. Hence, $\dot{V}_1$ and $\dot{V}_2$ are negative definite in the switching surfaces. Moreover, if $x_1(t = 0) \neq x_{1d}(t = 0)$ and $x_2(t = 0) \neq x_{2d}(t = 0)$, Eq. (15) shows that $S_1(x) = 0$ and $S_2(x) = 0$ will be reached in the finite times t_{1reach} and t_{2reach}, respectively.

It is clear that with starting from initial conditions, trajectories reach the manifold $S_1(x) = 0$ and $S_2(x) = 0$ in the finite times and slide toward the origins of the error phase planes according to Eq. (11). But, function $sign$ in Eq. (13) causes the high frequency switching near the sliding surfaces. Thus, in order to reduce this chattering phenomenon, the sign function is replaced with the saturation function as follows.

$$u_1 = \hat{u}_1 - K_1\, sat(S_1(x)b_1(x)\phi_1) \text{ and } K_1 > 0$$
$$u_2 = \hat{u}_2 - K_2\, sat(S_2(x)b_2(x)\phi_2) \text{ and } K_2 > 0 \tag{16}$$

which sat is the saturation function. ϕ_1 represents the inverse of the width of boundary layer for S_1. ϕ_2 represents the inverse of the width of boundary layer for S_2.

3.3 Decoupled Sliding Mode Control for Non-canonical Forms

The sliding mode control technique described in the previous section could not be applied to a system with the form of Eq. (10), which is not in the canonical form and includes the coupled subsystems. The basic idea of the decoupled sliding mode control is the design of a control law such that the single input u simultaneously controls several subsystems to accomplish the desired performance. To achieve this goal, the following sliding surfaces are defined.

$$S_1(x) = \lambda_1(x_2 - x_{2d} - z) + x_4 - x_{4d} = 0 \tag{17}$$
$$S_2(x) = \lambda_2(x_1 - x_{1d}) + x_3 - x_{3d} = 0 \tag{18}$$

where variable Z is used to transfer S_2 to S_1. Furthermore, its value is proportional to S_2 and its range is proper to x_2. Comparing Eq. (17) with (11) shows that the control objectives for the subsystem are $x_2 = x_{2d} + z$ and $x_4 = x_{4d}$. On the other hand, Eq. (18) means that the control objectives are $x_1 = x_{1d}$ and $x_3 = x_{3d}$. Now, let the control law for Eq. (17) be the sliding mode control with a boundary layer which is similar to Eq. (16):

$$u_1 = \hat{u}_1 - G_{f1}\, sat\,(S_1(x)b_1(x)G_{s1}) \text{ and } G_{f1}, G_{s1} > 0 \tag{19}$$
$$\text{with } \hat{u}_1 = -b_1^{-1}(x)\,(f_1(x) - \ddot{x}_{2d} + \lambda_1 x_4 - \lambda_1 \dot{x}_{2d}) \tag{20}$$

Sliding constant λ_1 is strictly positive. Now, let the control law for Eq. (18) be another sliding mode controller with a boundary layer as follows.

$$z = G_{f2}\, sat\,(S_2(x)G_{s2})\,, \text{ and } 0 < G_{f2} < 1 \tag{21}$$

Note that in (21), z is a decaying oscillation signal due to $0 < G_{f2} < 1$. Moreover, in Eq. (17), if $S_1 = 0$, then $x_2 = x_{2d} + z$ and $x_4 = x_{4d}$.

Therefore, the control sequence is as follows. When $S_2 \to 0$, then $z \to 0$ in Eq. (17), and it forces Eq. (19) to generate a controller action for reducing S_2; as S_2 decreases, z decreases too. Hence, at the limit $S_2 \to 0$ with $x_1 \to x_{1d}$, then $z \to 0$ with $x_2 \to x_{2d}$, so $S_1 \to 0$, and the goal will be achieved.

4 Biped Robot

4.1 The Dynamic Model of the Biped Robot

The robot is modeled in the lateral plane by using a three-link-planar model. Figure 1 shows the model of the robot. The first link is anchored to the ground surface, while the third link moves freely along the lateral plane and the second link represents the head, arms and trunk. Four characteristics of mass, length, inertia and the center of gravity are used to define each link. Anthropometric parameters are obtained from Winter (1990) for a humanoid model which is 171 cm in height and 74 kg in weight and are illustrated in Table 1. The distance between two legs of the model ($2d_2$) is equal to 32.7 cm.

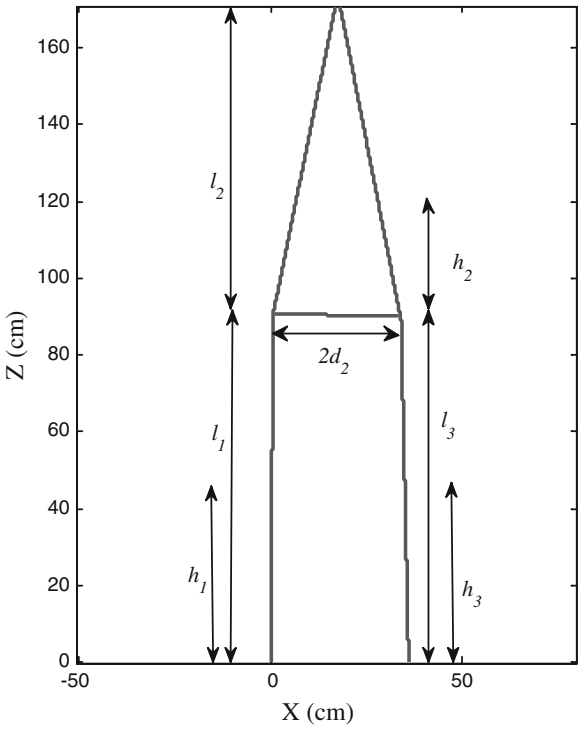

Fig. 1 The parameters of the robot based on the anthropometric table

Table 1 The anthropometric parameters of the model

	First link	Second link	Third link	Unit
Mass	$m_1 = 13.75$	$m_2 = 46.5$	$m_3 = 13.75$	kg
Inertia	$I_1 = 1.4$	$I_2 = 3.25$	$I_3 = 1.4$	$kg\,m^2$
Length	$l_1 = 0.91$	$l_2 = 0.8$	$l_3 = 0.91$	m
CG	$h_1 = 0.50$	$h_2 = 0.27$	$h_3 = 0.50$	m

The Newton-Euler method is employed to gain the dynamic equations of the model (Mahmoodabadi et al. 2014a, b). The dynamic equations of the model for θ_1, θ_2 and θ_3 are (Fig. 2):

$$\begin{aligned} I_1\ddot{\theta}_1 = {} & u_1 - u_2 + h_1 m_1 g \ \sin\theta_1 + l_1 \sin\theta_1 \ g \ (m_2 + m_3) \ + h_1 m_1 \left(-h_1 \ddot{\theta}_1\right) \\ & + l_1 m_2 \ [\ - \ddot{\theta}_1 l_1 + \ddot{\theta}_2 \{d_2 \sin(\theta_2 - \theta_1) - h_2 \cos(\theta_2 - \theta_1)\} + \dot{\theta}_2^2 \{d_2 \cos(\theta_2 - \theta_1) \\ & + h_2 \sin(\theta_2 - \theta_1)\}] \ + l_1 m_3 [-\ddot{\theta}_1 l_1 + \vec{\theta}_2 \{2d_2 \sin(\theta_2 - \theta_1) - \theta_3 \ (l_2 - h_3) \cos(\theta_3 - \theta_1) \\ & + \dot{\theta}_2^2 \ 2d_2 \cos(\theta_2 - \theta_1) + \dot{\theta}_3^2 \ (l_3 - h_3) \sin(\theta_3 - \theta_1)] \end{aligned} \tag{22}$$

$$\begin{aligned} I_2\ddot{\theta}_2 = {} & u_2 - u_3 + m_2 d_2 g \cos\theta_2 + m_2 h_2 g \sin\theta_2 + 2m_3 d_2 g \cos\theta_2 \\ & - \ddot{\theta}_1 \ [\cos(\theta_2 - \theta_1) m_2 h_2 l_1 - \sin(\theta_2 - \theta_1) m_3 2d_2 l_1 - \sin(\theta_2 - \theta_1) m_2 d_2 l_1] \\ & + \dot{\theta}_1^2 [\sin(\theta_1 - \theta_2) m_2 l_1 h_2 - \cos(\theta_2 - \theta_1) 2m_3 d_2 l_1 - \cos(\theta_2 - \theta_1) m_2 d_2 l_1] \\ & + \ddot{\theta}_2 [-m_2 d_2^2 - 4m_3 d_2^2 - m_2 h_2^2] + \ddot{\theta}_3 [2m_3 d_2 (l_3 - h_3) \sin(\theta_2 - \theta_3)] \\ & - \dot{\theta}_3^2 [2m_3 d_2 (l_3 - h_3) \cos(\theta_2 - \theta_3)] \end{aligned} \tag{23}$$

$$\begin{aligned} I_3\ddot{\theta}_3 = {} & (l_3 - h_3) \, m_3 g \sin\theta_3 + \ u_3 - m_3 \ (l_3 - h_3) \, l_1 \cos(\theta_3 - \theta_1) \ \ddot{\theta}_1 \\ & + m_3 \ (l_3 - \ h_3) \, l_1 \sin(\theta_1 - \theta_3) \ \dot{\theta}_1^2 + 2d_2 m_3 \ (l_3 - h_3) \sin(\theta_2 - \theta_3) \ \ddot{\theta}_2 \\ & + 2d_2 m_3 \ (l_3 - h_3) \cos(\theta_3 - \ \theta_2) \ \ddot{\theta}_2 - m_3 (l_3 - h_3)^2 \ddot{\theta}_3 \end{aligned} \tag{24}$$

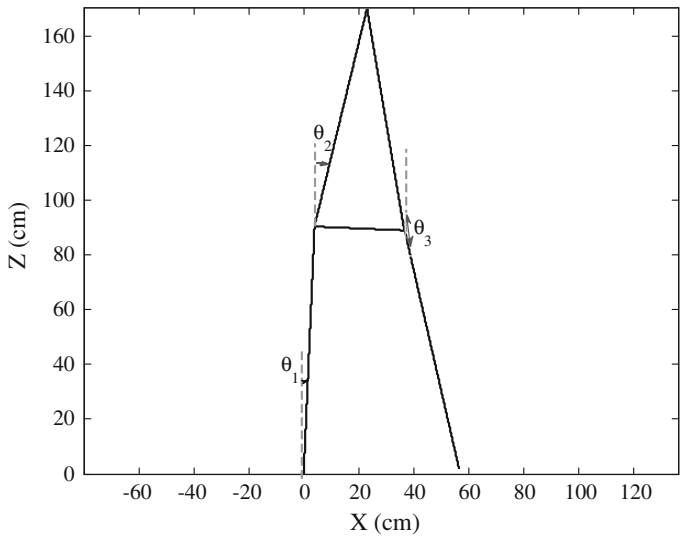

Fig. 2 The angles of the robot

The walking of biped robot in the lateral plane is periodic, and it can be divided into two phases (Mahmoodabadi et al. 2014a, b). These two phases are Double Support Phase (DSP) and Single Support Phase (SSP). DSP term is used for situations where the biped robot has two isolated contact surfaces with the floor. Indeed, this situation happens when the biped robot is supported by both feet. The time of this phase is regarded as 20 percent of the whole time. SSP term is employed for situations where the biped robot has only one contact surface with the floor. This situation occurs when the biped robot is supported with only one foot. According to Fig. 3, the biped robot passes DSP and SSP, respectively. The swing foot trajectory which has the first-order continuity is generated, and it maintains the ZMP on the inside of the support polygon. Then, the inverse kinematic is utilized to obtain the desired trajectories of the joints. The desired trajectories should have first-order and second-order continuity. The first-order derivative continuity guarantees smoothness of the joint velocity, while the second order continuity guarantees smoothness of the acceleration or torque on the joints (Mahmoodabadi et al. 2014a, b).

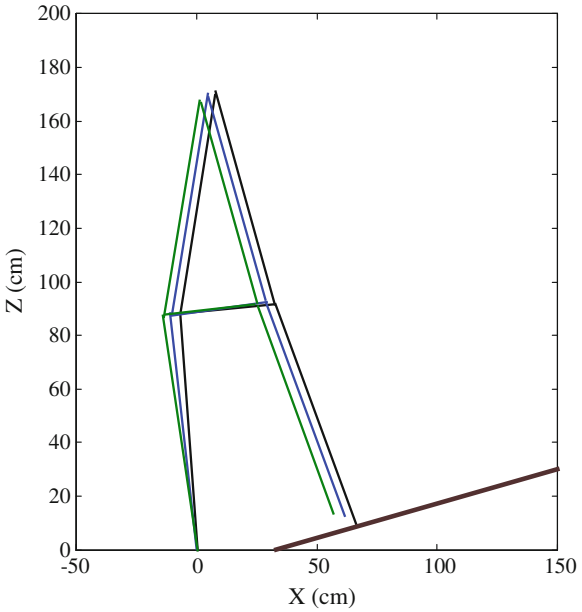

Fig. 3 The stick diagram of the biped robot walking in the lateral on slope

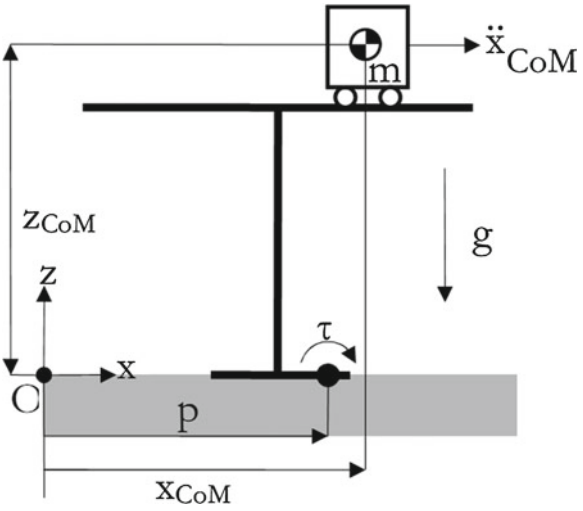

Fig. 4 Cart table model

If the biped robot's joint velocities augment, the dynamic forces will dominate the static forces. The faster the movements, the more dominate these dynamic forces will be. ZMP can be regarded as the dynamical equivalent of the Floor projection of the Center Of Mass (FCOM). The ZMP criterion does take dynamic forces, as well as static forces, into consideration. In order to achieve a dynamically stable gait, ZMP should be within on the inside of the support polygon at every time instance. The support polygon in DSP is the area between both feet. The support polygon i.e. x_{ZMP} in this problem ranges from -11.5 to 44.2 cm in the DSP and ranges from -11.5 to 11.5 cm in the SSP (Mahmoodabadi et al. 2014a, b). The cart-table model is used to compute the ZMP. Figure 4 illustrates the simplified model of the biped robot, which consists of a running cart on a mass-less table. The cart has mass m, and its position (x, z) corresponds to the equivalent center of the mass of the biped robot. The center of reference frame is considered in the middle of the stance foot. Moreover, the table is assumed to have the same support polygon as the biped robot. The torque around point p can be written as (Mahmoodabadi et al. 2014a, b):

$$\tau = -mg\,(x_{CoM} - p) + m\ddot{x}_{CoM} z_{CoM} \tag{25}$$

g is the gravitational acceleration downwards. Now, using the ZMP definition: torque must be zero and, thus $x_{ZMP} = p$, we have:

$$x_{ZMP} = p = x_{CoM} - \frac{\ddot{x}_{CoM}}{g} z_{CoM} \tag{26}$$

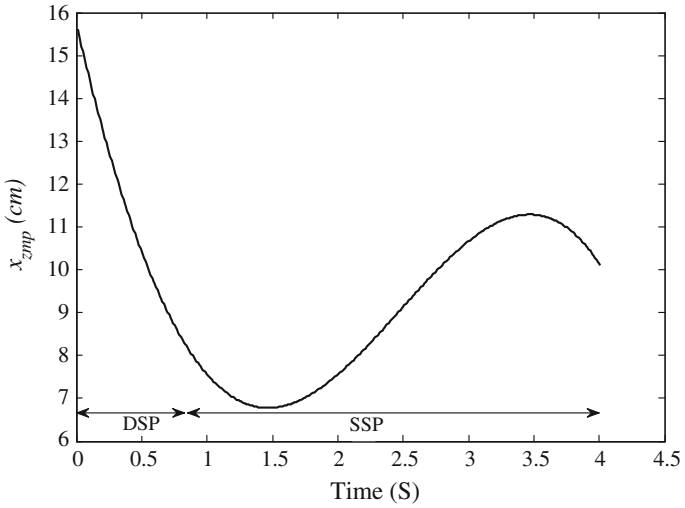

Fig. 5 Zero moment point on the inside of support polygon

The robot tracks the desired trajectories and maintains the ZMP on the inside of the support polygon, simultaneously (Fig. 5).

4.2 Sliding Mode Control for the Biped Robot

The sliding mode controller has been successfully employed to control the robots (Jing and Wuan 2006). Islam et al. applied multiple model/control-based sliding mode control to a 2-DOF robot manipulator (Islam and Liu 2011). Xiuping et al. controlled a biped robot in the double support phase by sliding mode control (Xiuping and Qiong 2004). Moosavian et al. controlled the biped robot in the sagittal plane with aid of sliding mode control and utilized the fuzzy system to regulate major control parameters (Moosavian et al. 2007). In the present chapter, there are six controlling coefficients, three sliding surfaces (s_i), and three equivalent control inputs(u_{eqi}), which must be chosen appropriately. The linear dynamic equations are utilized to obtain the equivalent control inputs u_{eqi} and $i = 1, 2, 3$ (appendix). Since the problem has three system states, the sliding surfaces and control inputs can be written, as follows:

$$s_i\,(e_i, t) = \left(\frac{d}{dt} + \lambda_i\right)^{n-1} e_i = 0 \qquad i = 1, 2 \text{ and } 3 \tag{27}$$

$$u_i = u_{eqi} - k_i \text{sat}\,(\Phi) \qquad i = 1, 2 \text{ and } 3 \tag{28}$$

4.3 The Pareto Design of Sliding Mode Control for the Biped Robot

The objective of the sliding mode control method is to define asymptotically stable surfaces in such a manner that all system trajectories converge to these surfaces and slide along them until reaching the origin at their intersection (Utkin 1978). However, the heuristic sliding parameters are required to be chosen properly. Hence, the multi-objective periodic CDPSO (Mahmoodabadi et al. 2011, 2012a), Sigma method (Mostaghim and Teich 2003), and modified NSGAII (Atashkari et al. 2007) are utilized to ascertain the proper parameters and eliminate the tedious and repetitive trial-and-error process. The performance of a controlled closed loop system is usually evaluated by a variety of goals (Toscana 2005; Wolovich 1994). In this chapter, normalized summation of angles errors and normalized summation of control effort are regarded as the objective functions. These objective functions have to be minimized simultaneously. The vector $[k_1, k_2, k_3, \lambda_1, \lambda_2, \lambda_3]$ is the vector of selective parameters of sliding mode control. k_1, k_2 and, k_3 are positive constants. λ_1, λ_2 and, λ_3 are coefficients of the sliding surfaces. The normalized summation of angles errors and normalized summation of control effort are functions of this vector's components. That is to say, we can make changes in the normalized summation of angles errors and normalized summation of control effort by choosing various values for the selective parameters. This is noticeably an optimization problem with two objective functions (normalized summation of angles errors and normalized summation of control effort) and six decision variables ($k_1, k_2, k_3, \lambda_1, \lambda_2, \lambda_3$). The regions of the selective parameters are:

k_1, k_2, k_3 : Positive constants $0 \leq k_1, k_2, k_3 \leq 10$

$\lambda_1, \lambda_2, \lambda_3$: Coefficients of the sliding surfaces $100 \leq \lambda_1, \lambda_2, \lambda_3 \leq 1000$

The parameters of the multi-objective periodic CDPSO algorithm are selected as follows. In each period, the inertia weight W is linearly decreased from $W_1 = 0.9$ to $W_2 = 0.4$, C_1 is linearly decreased from $C_{1i} = 2.5$ to $C_{1f} = 0.5$, and C_2 is linearly increased from $C_{2i} = 0.5$ to $C_{2f} = 2.5$, over time. The related variables used in the convergence and divergence operators are: $P_{Convergence} = 0.1$, $P_{Divergence} = 0.1$, and $S_D = \frac{x_{max} - x_{min}}{2}$. The term v" is limited to the range of $[-v_{ave}, +v_{ave}]$, in which $v_{ave} = \frac{x_{max} - x_{min}}{2}$. While the velocity violates this range, it will be multiplied by a random number between [0, 1]. Furthermore, the positive constant for $\varepsilon_{elimination}$ is $\zeta = 300$ and the neighborhood radius for the leader selection is $R_{neighborhood} = 0.04$. The number of iterations in a period equals $T = 7$, the swarm size is 50 and the maximum iteration equals 150. The Pareto front of multi-objective periodic CDPSO (Mahmoodabadi et al. 2011, 2012a) for this issue is shown in Fig. 6, and multi-objective periodic CDPSO's feasibility and efficiency is assessed in comparison with Sigma method (Mostaghim and Teich 2003) and modified NSGAII (Atashkari et al. 2007).

Although the functioning of these algorithms is competitively appropriate in the present chapter, the most interesting result is that the multi-objective periodic CDPSO algorithm has more uniformity and diversity. In Fig. 6, points A and C stand for the

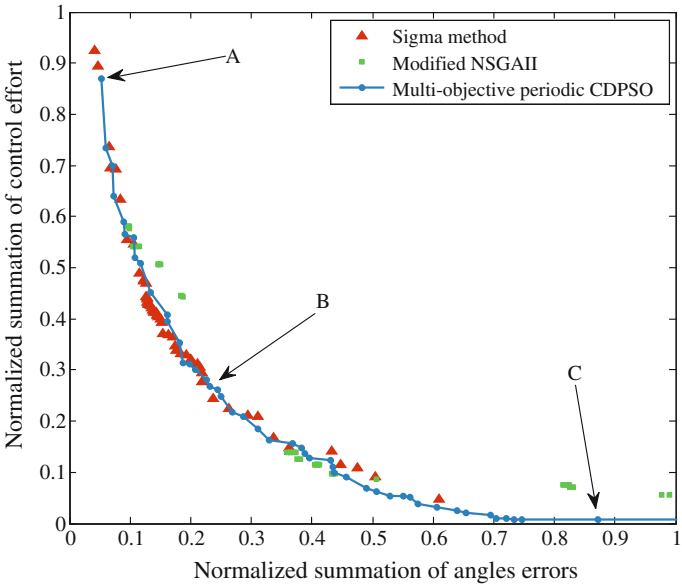

Fig. 6 The obtained Pareto fronts obtained by using Sigma method (Mostaghim and Teich 2003), modified NSGAII (Atashkari et al. 2007), and multi-objective periodic CDPSO (Mahmoodabadi et al. 2011, 2012a) for optimal control design of the biped robot

best normalized summation of angles errors and normalized summation of control effort, respectively. According to this figure, all the optimum design points in the Pareto front are non-dominated and can be selected by the designer as optimal sliding mode tracking controllers. Furthermore, choosing a better value for any objective function in the Pareto front causes a worse value for another objective. The corresponding decision variables (vector of sliding mode tracking controllers) of the Pareto front shown in Fig. 6 are the best possible design points. In this regard, if any other set of decision variables is chosen, the corresponding values of the pair of those objective functions will place an inferior point in Pareto front. Indeed, the inferior area in the space of the two objective functions is top/right side of Fig. 6. Hence, there are some crucial optimal design facts between these two objective functions which have been ascertained by the Pareto optimum design approach. Point B in Fig. 6 demonstrates important optimal design facts; in fact, it can be the trade-off optimum choice when considering minimum values of both of the normalized summation of angles errors and normalized summation of control effort. Design variables and objective functions according to theoptimum design points A, B, and C are illustrated

in Table 2. The real tracking trajectories of the optimum design points A, B, and C are shown in Figs. 7, 8 and 9. The tracking error of the optimum design points A, B, and C are shown in Figs. 10, 11 and 12. In addition, Figs. 13, 14 and 15 illustrate the sliding surfaces of the optimum design points A, B, and C.

Table 2 The objective functions and their associated design variables for the optimum points of Fig. 6

Optimum design point	A	B	C
Normalized summation of angles errors	5.18×10^{-2}	2.44×10^{-1}	8.72×10^{-1}
Normalized summation of control effort	8.69×10^{-1}	2.61×10^{-1}	8.30×10^{-3}
Design variable k_1	7.04×10^{-2}	3.71×10^{0}	1.98×10^{0}
Design variable k_2	3.54×10^{-5}	6.69×10^{-5}	7.75×10^{-2}
Design variable k_3	6.53×10^{-3}	1.59×10^{-3}	8.24×10^{-1}
Design variable λ_1	5.76×10^{2}	2.24×10^{2}	1.00×10^{2}
Design variable λ_2	5.98×10^{2}	2.60×10^{2}	1.01×10^{2}
Design variable λ_3	6.02×10^{2}	2.54×10^{2}	1.00×10^{2}

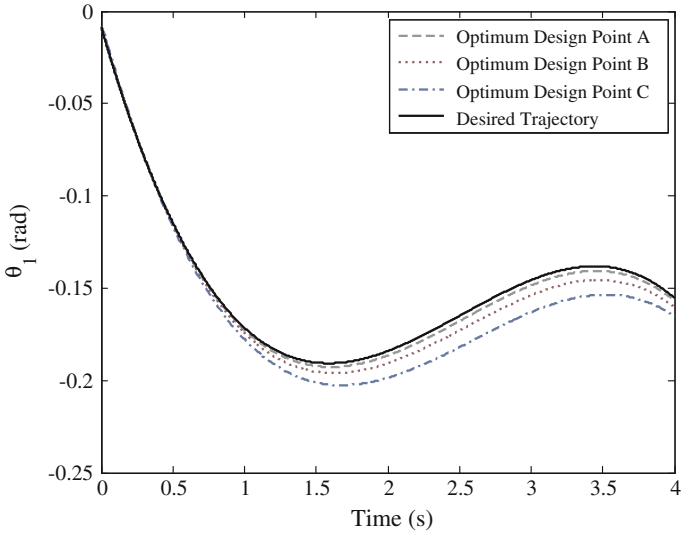

Fig. 7 The tracking trajectory θ_1 of the optimum design points A, B, and C shown in the Pareto front (Fig. 6)

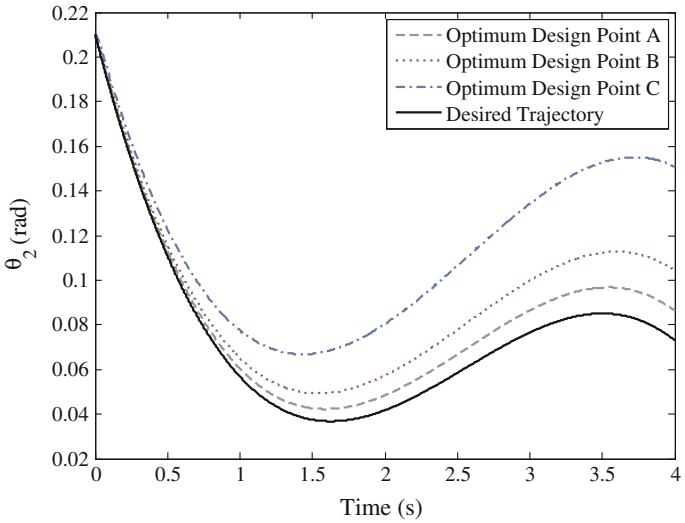

Fig. 8 The tracking trajectory θ_2 of the optimum design points A, B, and C shown in the Pareto front (Fig. 6)

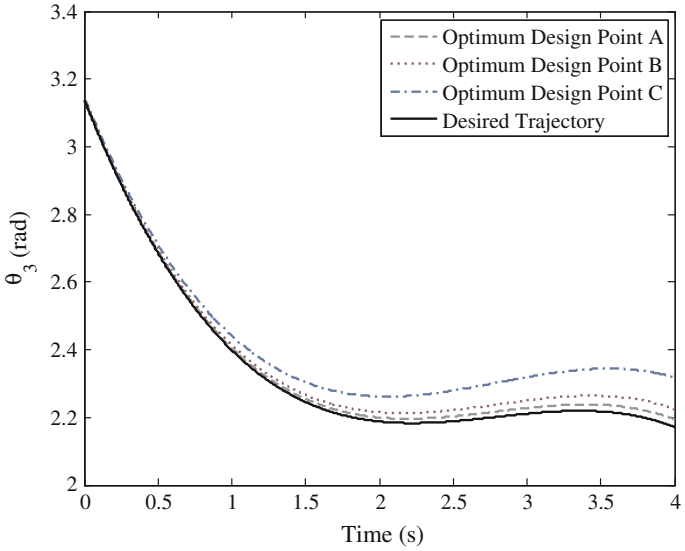

Fig. 9 The tracking trajectory θ_3 of the optimum design points A, B, and C shown in the Pareto front (Fig. 6)

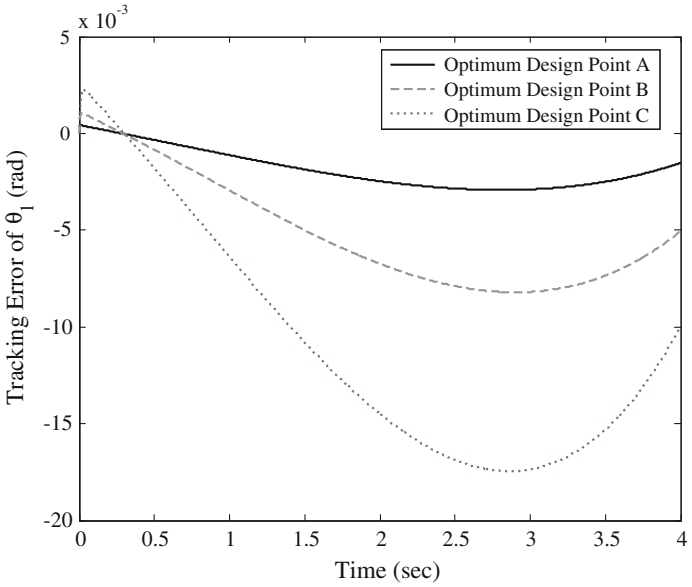

Fig. 10 The tracking error of θ_1 for the optimum design points A, B, and C shown in the Pareto front (Fig. 6)

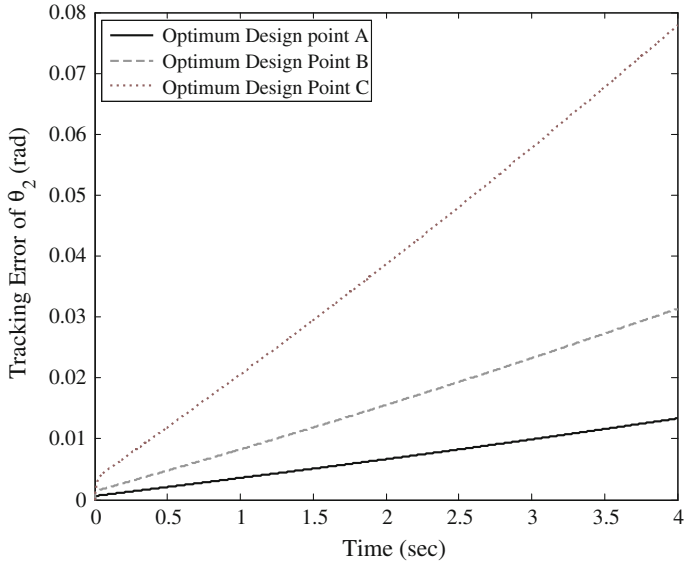

Fig. 11 The tracking error of θ_2 for the optimum design points A, B, and C shown in the Pareto front (Fig. 6)

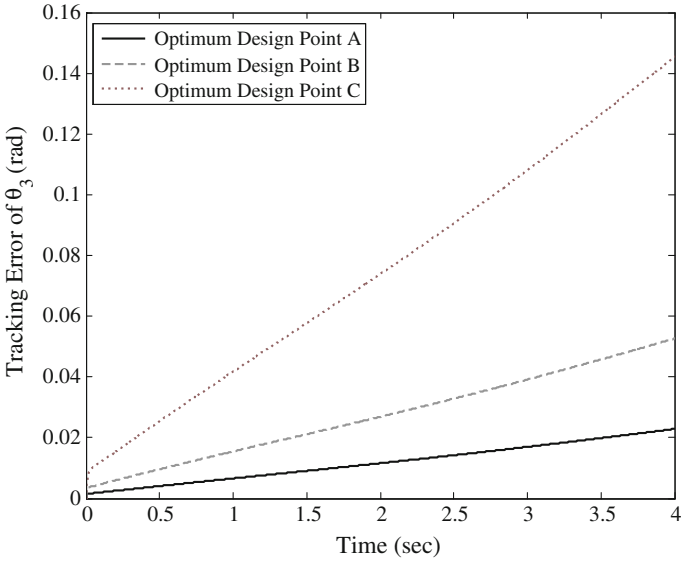

Fig. 12 The tracking error of θ_3 for the optimum design points A, B, and C shown in the Pareto front (Fig. 6)

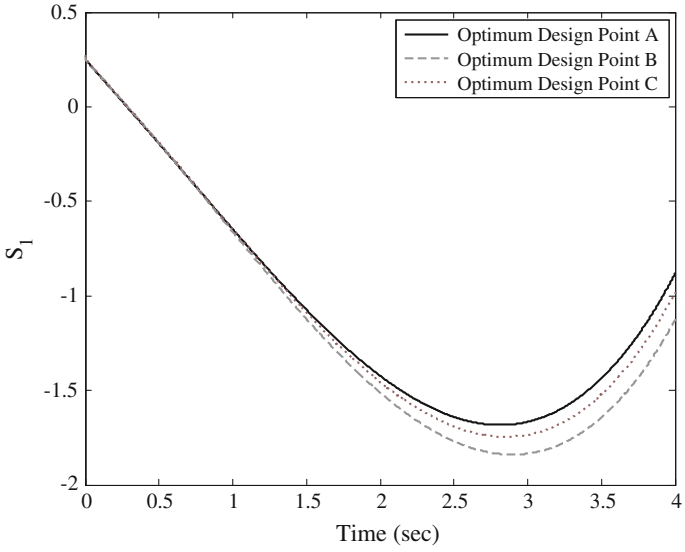

Fig. 13 The sliding surface S_1 of the optimum design points A, B, and C shown in the Pareto front (Fig. 6)

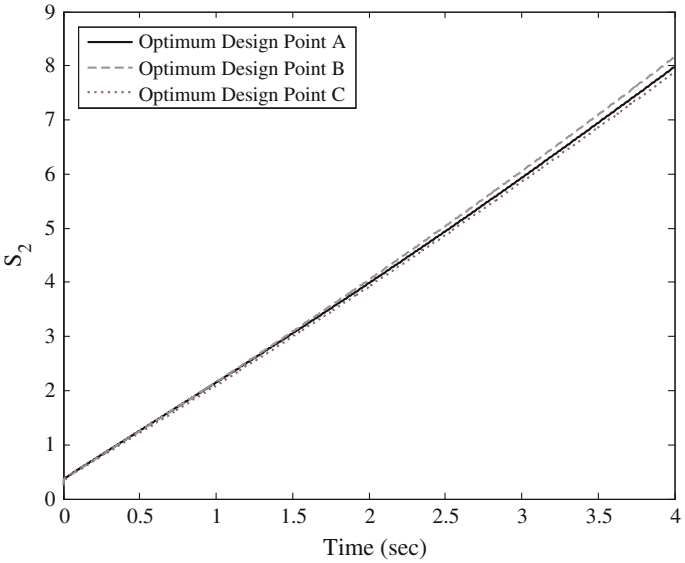

Fig. 14 The sliding surface S_2 of the optimum design points A, B, and C shown in the Pareto front (Fig. 6)

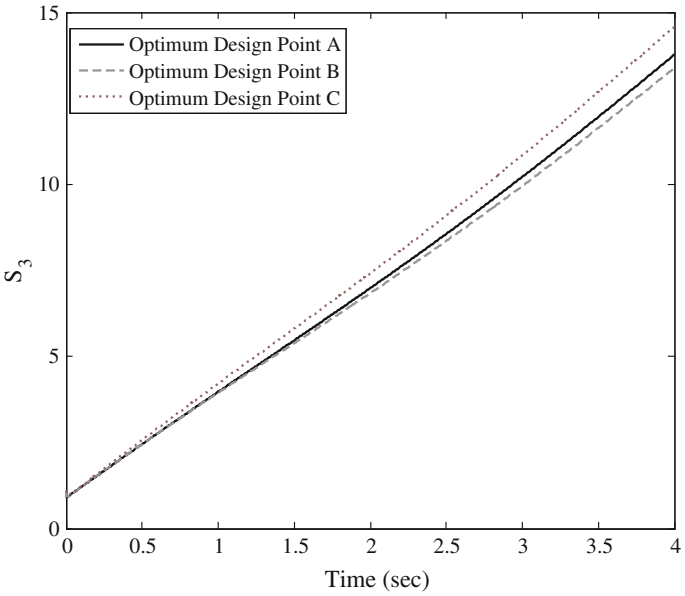

Fig. 15 The sliding surface S_3 of the optimum design points A, B, and C shown in the Pareto front (Fig. 6)

5 The Ball and Beam System

5.1 The Dynamic Model of the Ball and Beam System

The ball and beam system is one of the most enduringly popular and important laboratory models for teaching control systems engineering (Fig. 16). The ball and beam is widely used to challenge the control techniques since it is very simple to understand as a system, its open loop system is unstable, and the control techniques of studying it include many important classical and modern design methods.

As shown in Fig. 16, a steel ball is rolling on the top of a long beam. The beam is mounted on the output shaft of an electrical motor and the beam can be tilted about its center axis by applying an electrical control signal to the motor amplifier. The control goal is to regulate the position of the ball on the beam by changing the angle of the beam. This is a difficult control task because the ball does not stay in one place on the beam and moves with acceleration that is approximately proportional to the tilt of the beam. In the control terminology, the open loop system is unstable because the system output (the ball position) increases without limit for a fixed input (beam angle). Feedback control must be used to stabilize the system and keep the ball in a desired position on the beam. In other words, the goal of the control approach is to control the torque u applied at the pivot of the beam, such that the ball can roll on the beam and track a desired trajectory. Hence, the torque causes a change in the angle of the beam and a movement in the position of the ball. By using of the Lagrangian method, the equations of motion are obtained as follows.

$$\left(I_b + m_s r^2\right)\ddot{\theta} + 2m_s r\dot{r}\dot{\theta} + m_s gr\cos\theta = u \tag{29}$$

$$\ddot{r} + \frac{5}{7}\left(g\sin\theta - r\dot{\theta}^2\right) = 0 \tag{30}$$

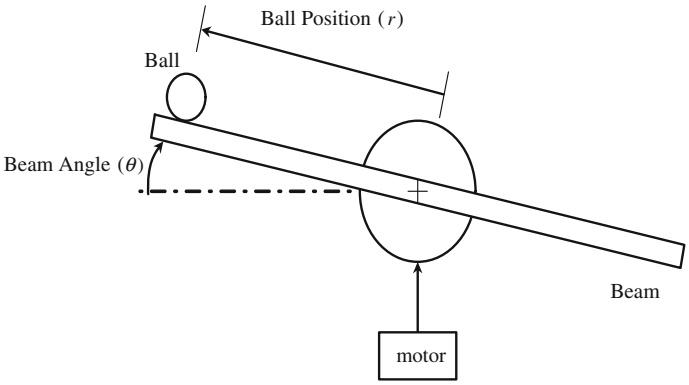

Fig. 16 The schematic model of the ball and beam system

where u is the torque applied to the beam, $I_b = \frac{m_b a^2}{12}$ is beam's moment of inertia, $m_b = 1\,\text{kg}$ is mass of beam, $a = 1\,\text{m}$ is the length of the beam , θ is the angle of the beam, $m_s = 0.05\,\text{kg}$ is the mass of the ball, I_s is the ball's moment of inertia ($I_s = \frac{2}{5}\left(m_s r_s^2\right)$), $r_s = 0.01\,\text{m}$ is the radius of the sphere, r stands for the position of the ball. If the states are defined as follows,

$$x_1 = \theta \quad , \quad x_2 = \dot{\theta} \quad , \quad x_3 = r \quad , \quad x_4 = \dot{r}$$

Then, the state-space equations would be written as Eq. (31).

$$\begin{cases} \dot{x}_1 = x_2 \\ \dot{x}_2 = \frac{-m_s x_3 (2x_4 x_2 - g\cos(x_1))}{m_s x_3^2 + I_b} + \frac{u}{m_s x_3^2 + I_b} \\ \dot{x}_3 = x_4 \\ \dot{x}_4 = -\frac{5}{7}\left(g\sin(x_1) - x_3 x_2^2\right) \end{cases} \tag{31}$$

5.2 Decoupled Sliding Mode Control for the Ball and Beam System

The optimal decoupled sliding mode controller has been successfully employed by researchers to control the ball and beam system. Alfaro-Cid et al. used the genetic algorithm to design the decoupled sliding mode controllers (Alfaro-Cid et al. 2005). Chang et al. designed optimal fuzzy sliding-mode control for the ball and beam system using fuzzy ant colony optimization (Chang et al. 2012). In Mahmoodabadi et al. (2012a), a multi-objective genetic algorithm was applied to Pareto design of decoupled sliding-mode controllers for nonlinear systems. In (Andalib Sahnehsaraei et al. 2013), multi-objective particle swarm optimization was utilized to design the decoupled sliding mode controller for an inverted pendulum system. Mahmoodabadi et al. proposed an online optimal decoupled sliding mode controller using the moving least squares and particle swarm optimization (Mahmoodabadi et al. 2014c). Regarding the DSMC of the ball and beam system in this chapter, the sliding surfaces can be written as follows:

$$S_1 = c_1(\theta - z) + \dot{\theta} = c_1(x_1 - z) + x_2 \tag{32}$$

$$S_2 = c_2 r + r = c_2 x_3 + x_4 \tag{33}$$

which

$$z = sat\left(\frac{S_2}{\varphi_2}\right) z_u \quad 0 < z_u < 1 \tag{34}$$

By using the decoupled sliding mode control strategy, we have:

$$\dot{S}_1 = c_1 x_2 - c_1 \dot{z} + f_1 + b_1 u_1 \tag{35}$$

which

$$\begin{cases} \dot{z} = 0 & if \quad \left|\frac{S_2}{\varphi_2}\right| \geq 1 \\ \dot{z} = \frac{z_u}{\varphi_2}\, \dot{S}_2 & if \quad \left|\frac{S_2}{\varphi_2}\right| < 1 \end{cases} \tag{36}$$

Furthermore

$$\dot{S}_2 = c_2\, \dot{x}_3 + \dot{x}_4 = c_2\, x_4 + f_2 + b_2\, u \tag{37}$$

$\hat{u}$ would be achieved if $\dot{S}_1 = 0$,

$$\begin{cases} \dot{S}_1 = c_1\, x_2 - \frac{c_1\, z_u}{\varphi_2}\,(c_2 x_4 + f_2 + b_2 u) + f_1 + b_1 u = 0 & if \quad \left(\frac{S_2}{\varphi_2}\right) < 1 \\ \dot{S}_1 = c_1\, x_2 + f_1 + b_1 u = 0 & if \quad \left(\frac{S_2}{\varphi_2}\right) \geq 1 \end{cases} \tag{38}$$

Therefore

$$\begin{cases} \hat{u} = \frac{-1}{b_1 - \frac{c_1 z_u}{\varphi_2} b_2} \left[f_1 + c_1\, x_2 - \frac{c_1 z_u}{\varphi_2}\,(f_2 + c_2 x_4) \right] & if \quad \left(\frac{S_2}{\varphi_2}\right) < 1 \\ \hat{u} = \frac{-1}{b_1}\,(f_1 + c_1\, x_2) & if \quad \left(\frac{S_2}{\varphi_2}\right) \geq 1 \end{cases} \tag{39}$$

and

$$u = \hat{u} - k\, sat\left(\frac{S_1\, b_1\,(x)}{\varphi_1}\right) \tag{40}$$

5.3 The Pareto Design of Decoupled Sliding Mode Control for the Ball and Beam System

In this section, the CDPSO approach is employed to select the parameters of DSMC for the ball and beam system with respect to two objective functions. To compare the performance of the optimizer technique, the optimization process is also performed via Sigma method (Mostaghim and Teich 2003) and modified NSGAII (Atashkari et al. 2007). The performance of a controlled closed-loop system is evaluated by various goals. In this chapter, the normalized integral of the absolute value of the ball distance and the normalized integral of the absolute value of the beam are considered as the objective functions. In other words, the objective functions and constrains are as follows:

Constraint: $\max(abs(u)) \leq 40\,N\,m$
Objective functions:

$$f_1 = \text{Normalized}\left(\int |r(t)|dt\right) \text{ and } f_2 = \text{Normalized}\left(\int |\theta(t)|dt\right)$$

These objective functions have to be minimized simultaneously. When solving the optimization problem, the population size and maximum iteration are set at 50 and 150, respectively. Vector $[c_1,\ c_2,\ \varphi_1,\ \varphi_2, k,\ z_u]$ is the vector of the selective parameters (design variables) of the decoupled sliding mode control.

In this chapter, we are concerned with choosing values for the selective parameters to minimize the objective functions. Clearly, this is an optimization problem with two object functions and six decision variables.

Now, it is supposed that the initial values for the states of the ball and beam system are as follows.

$$\left(x_1 = \frac{\pi}{3}\ ,\ \ x_2 = 0\ ,\ \ \ x_3 = 0.1\ ,\ \ \ x_4 = 0\right) \tag{41}$$

The regions of the selective parameters are:

$$1 \leq c_1 \leq 100,\quad 0.3 \leq c_2 \leq 10,\quad 1 \leq \varphi_1 \leq 100,\quad 0.01 \leq \varphi_2 \leq 1,\quad 0 \leq k \leq 10,\quad 0.1 \leq z_u \leq 1$$

The parameters of the multi-objective periodic CDPSO algorithm are chosen as follows. In each period, the inertia weight W is linearly decreased from $W_1 = 0.9$ to $W_2 = 0.4$, C_1 is linearly decreased from $C_{1i} = 2.5$ to $C_{1f} = 0.5$, and C_2 is linearly increased from $C_{2i} = 0.5$ to $C_{2f} = 2.5$, over time. The related variables used in the convergence and divergence operators are: $P_{Convergence} = 0.1$, $P_{Divergence} = 0.1$, and $S_D = \frac{x_{max} - x_{min}}{2}$. The term v" is limited to the range of $[-v_{ave}, +v_{ave}]$, in which $v_{ave} = \frac{X_{max} - X_{min}}{2}$. While the velocity violates this range, it will be multiplied by a random number between [0, 1]. Furthermore, the positive constant for $\varepsilon_{elimination}$ is $\zeta = 300$ and the neighborhood radius for leader selection is $R_{neighborhood} = 0.04$. The number of iterations in a period is equal to $T = 7$, the swarm size is 50 and the maximum iteration is equal to 150. The Pareto front of multi-objective periodic CDPSO (Mahmoodabadi et al. 2011, 2012a) for this problem is shown in Fig. 17, and multi-objective periodic CDPSO's feasibility and efficiency are assessed in comparison with Sigma method (Mostaghim and Teich 2003) and modified NSGAII (Atashkari et al. 2007).

In Fig. 17, points A and C stand for the best normalized integral of the absolute value of the ball distance and the normalized integral of the absolute value of the beam angle, respectively. According to this figure, the multi-objective periodic CDPSO algorithm has more uniformity and diversity in comparison to Sigma method (Mostaghim and Teich 2003) and modified NSGAII (Atashkari et al. 2007). Moreover, all the optimum design points in the Pareto front are non-dominated and can be chosen by the designer as optimal decoupled sliding mode controllers. It is noticeable

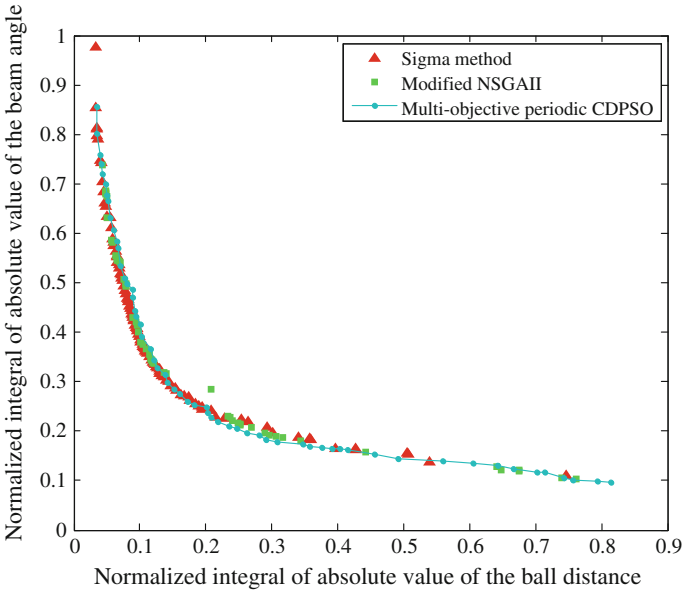

Fig. 17 The obtained Pareto fronts by using Sigma method (Mostaghim and Teich 2003), modified NSGAII (Atashkari et al. 2007), and multi-objective periodic CDPSO (Mahmoodabadi et al. 2011, 2012a) for optimal control design of the ball and beam system

Table 3 The objective functions and their associated design variables for the optimum points of Fig. 17

	c_1	c_2	φ_1	φ_2	k	z_u	f_1	f_2
Point A	5.8655	1.7532	20.2309	0.9514	0.6817	0.8729	0.0353	0.8561
Point B	30.648	1.9889	43.0080	0.2075	0.7272	0.7370	0.2919	0.1832
Point C	4.8042	1.6336	32.0405	0.9434	0.0266	0.4044	0.8143	0.0975

that choosing a better value for any objective function in the Pareto front causes a worse value for another objective function. Point B in Fig. 17 demonstrates important optimal design facts. This point can be the trade-off optimum choice when considering minimum values of both of the normalized integral of the absolute value of the ball distance and the normalized integral of the absolute value of the beam angle. Design variables and objective functions according to the optimum design points A, B, and C are illustrated in Table 3. The response time of the ball and beam system for the optimum design points A, B, and C are shown in Figs. 18, 19 and 20.

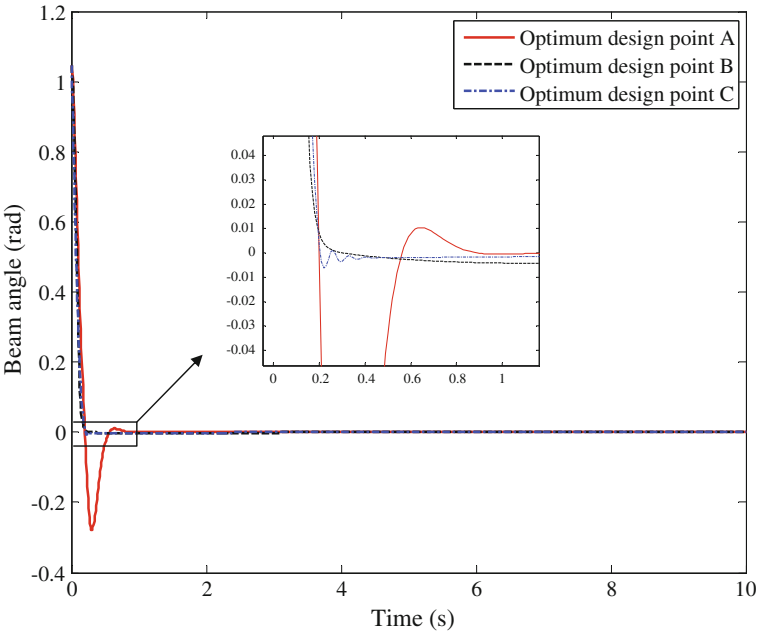

Fig. 18 The time response of the beam angle for the optimum design points A, B, and C shown in the Pareto front (Fig. 17)

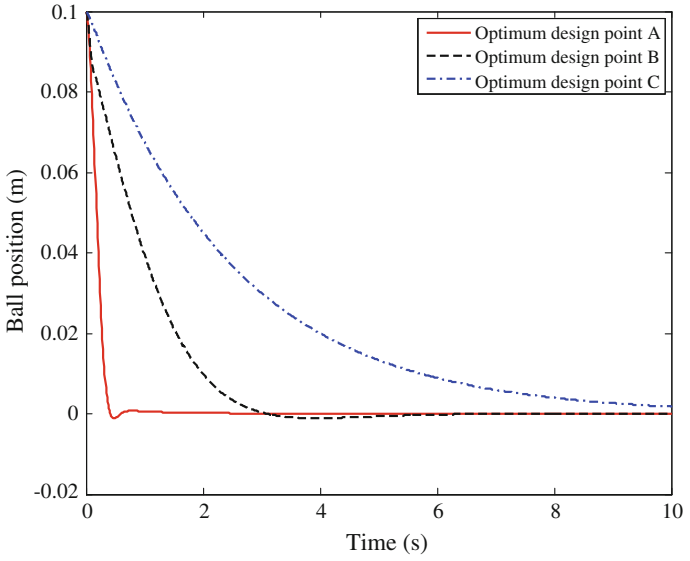

Fig. 19 The time response of the ball distance of the optimum design points A, B, and C shown in the Pareto front (Fig. 17)

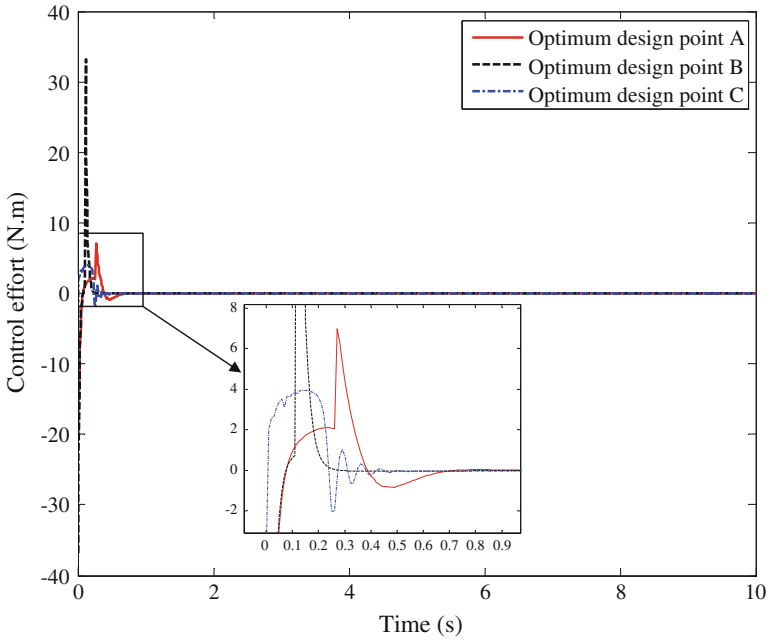

Fig. 20 The time response of the control effort for the ball and beam system of the optimum design points A, B, and C shown in the Pareto front (Fig. 17)

6 Conclusions

This chapter described two optimal control problems. First, the optimal sliding mode tracking control was introduced for a biped robot stepping in the lateral plane on slope. Both single support phase and double support phase were considered to take the ZMP on the inside of the support polygon. Second, the optimal decoupled sliding mode control was introduced for a ball and beam system. To this end, the multi-objective periodic CDPSO algorithm was used to acquire the Pareto front of the non-commensurable objective functions in the design of the SMC and DSMC. Two conflicting objective functions for the biped robot are the normalized summation of angles errors and normalized summation of control effort. Also, the conflicting objective functions for the ball and beam system are the normalized integral of the absolute value of the ball position and the normalized integral of the absolute value of the beam angle. After applying multi-objective periodic CDPSO, modified NSGAII and Sigma method to the design of an optimal controller for these problems, the Pareto fronts of multi-objective periodic CDPSO were compared with the Pareto fronts of modified NSGAII and Sigma method. The Pareto fronts of multi-objective periodic CDPSO were much more scattered than the other two algorithms. Hence, the designer has the ample opportunity to select the finest points. Finally, three points of each Pareto front of multi-objective periodic CDPSO were selected to compute

the parameters of the SMC and DSMC. The results demonstrated the efficacy of multi-objective periodic CDPSO in the design of the SMC and DSMC for problems with challenging dynamic equations.

Acknowledgments The authors would like to thank the anonymous reviewers for their valuable suggestions that enhance the technical and scientific quality of this chapter.

Appendix

The equivalent sliding mode control inputs for the biped robot are as follows

$$\begin{aligned} u_{eq1} = {} & -0.2260855175\,\dot{\theta}_2 - 5.376931543\,\theta_3 + 0.5609845516t^3 - 24.77733929t \\ & + 11.04563973 + 0.3042022263\dot{\theta}_3 - 52.53069026\theta_1 \\ & - 23.33466928\lambda_2\dot{\theta}_2 - 2.116394625\lambda_3\dot{\theta}_3 - 61.09883670\lambda_1\dot{\theta}_1 \\ & + 1.093385806\dot{\theta}_1 - 2.335441469\lambda_3 - 5.878003190\lambda_2 \\ & - 16.56389463\lambda_1 - 14.61433450\theta_2 - 1.029058915\lambda_2 t^2 \\ & + 5.282969124\ \lambda_2 t + 11.12677748t^2 - 0.3123798467\lambda_3 t^2 \\ & + 1.744755729\lambda_3 t - 3.024392417\lambda_1 t^2 + 15.22583011\lambda_1 t \end{aligned}$$

$$\begin{aligned} u_{eq2} = {} & 2.127074613\left(10^{-10}\right)\dot{\theta}_2 + 3.014817654\theta_3 - 0.1832721690t^3 \\ & - 7.435154298t + 0.06684314392\dot{\theta}_3 + 0.60810825555\theta_1 \\ & - 12.97075008\lambda_2\dot{\theta}_2 - 2.116394625\lambda_3\dot{\theta}_3 - 6.759058956\lambda_1\dot{\theta}_1 \\ & + 1.093385810\dot{\theta}_1 - 2.335441469\lambda_3 - 3.267331946\lambda_2 \\ & - 1.832380883\lambda_1 - 14.19340124\theta_2 - 0.5720100787\lambda_2 t^2 \\ & + 2.936577819\lambda_2 t + 3.182845520t^2 + 9.317127676 \\ & - 0.3123798467\lambda_3 t^2 + 1.744755729\lambda_3 t - 0.3345734183\lambda_1 t^2 \\ & + 1.684357492\lambda_1 t \end{aligned}$$

$$\begin{aligned} u_{eq3} = {} & -3.400956231\left(10^{-11}\right)\dot{\theta}_2 + 3.029347274\theta_3 - 0.2748341166t^3 \\ & - 3.658549547t + 11.95619521 + 1.750512761\left(10^{-10}\right)\dot{\theta}_3 \\ & + 0.12935207410\theta_1 - 2.497500599\lambda_2\dot{\theta}_2 - 3.630907800\lambda_3\dot{\theta}_3 \\ & + 3.604860241\lambda_1\dot{\theta}_1 + 0.2233967865\dot{\theta}_1 - 4.006706757\ \lambda_3 \\ & - 0.6291204009\ \lambda_2 + 0.9772776114\lambda_1 + 1.33021167t^2 \\ & - 0.01647731197\theta_2 - 0.1101397764\ \lambda_2 t^2 + 0.5654341356\lambda_2 t \\ & - 0.8983311722\ \lambda_1 t - 0.5359219913\ \lambda_3 t^2 + 2.993320390\ \lambda_3 t \\ & + 0.1784405819\lambda_1 t^2 \end{aligned}$$

References

Adhikary, N., Mahanta, C.: Integral backstepping sliding mode control for underactuated systems: swing-up and stabilization of the cart-pendulum system. ISA Trans. **52**(6), 870–880 (2013)

Alfaro-Cid, E., McGookin, E.W., Murray-Smith, D.J., Fossen, T.I.: http://www.sciencedirect.com/science/article/pii/S0967066104001741Genetic algorithms optimisation of decoupled sliding mode controllers: simulated and real results. Control Eng. Pract. 13(6), 739–748 (2005)

Andalib Sahnehsaraei, A., Mahmoodabadi, M.J., Taherkhorsandi, M.: Optimal robust decoupled sliding mode control based on a multi-objective genetic algorithm. In: Proceedings of International Symposium on Innovations in Intelligent Systems and Application, Albena, 19–21 June 2013, pp. 1–5 doi:10.1109/INISTA.2013.6577641

Angeline, P.J.: Using selection to improve particle swarm optimization. Proceedings of Congress on Evolutionary Computation, Anchorage 4–9 May 1998, pp. 84–89 doi:10.1109/ICEC.1998.699327

de Aparecida, P.A., Horst Albrecht, C., de Souza Leite Pires, L.B., Pinheiro Jacob, B.: Tailoring the particle swarm optimization algorithm for the design of offshore oil production risers. Optim. Eng. **12**(1–2), 215–235 (2011)

Atashkari, K., Nariman-Zadeh, N., Golcu, M., Khalkhali, A., Jamali, A.: Modelling and multi-objective optimization of a variable valve-timing spark-ignition engine using polynomial neural networks and evolutionary algorithms. Energy Convers. Manag. **48**(3), 1029–1041 (2007)

Aziz, A.S.A., Azar, A.T., Salama, M.A., Hassanien, A.E., Hanafy, S.E.O.: Genetic algorithm with different feature selection techniques for anomaly detectors generation. Proceedings of Federated Conference On Computer Science And Information Systems Kraków, 8–11 Sept 2013, pp. 769–774

Basin, M., Rodriguez-Ramirez, P., Ferrara, A., Calderon-Alvarez, D.: Sliding mode optimal control for linear systems. J. Franklin Inst. **349**(4), 1350–1363 (2012)

Bayramoglu, H., Komurcugil, H.: Time-varying sliding-coefficient-based terminal sliding mode control methods for a class of fourth-order nonlinear systems. Nonlinear Dyn. **73**(3), 1645–1657 (2013)

Belmecheri, F., Prins, C., Yalaoui, F., Amodeo, L.: Particle swarm optimization algorithm for a vehicle routing problem with heterogeneous fleet, mixed backhauls, and time windows. J. Intell. Manuf. **24**(4), 775–789 (2013)

Biswas, S., Mandal, K.K., Chakraborty, N.: Constriction factor based particle swarm optimization for analyzing tuned reactive power dispatch. Front. Energy **7**(2), 174–181 (2013)

De Carvalho, A.B., Pozo, A.: Measuring the convergence and diversity of CDAS multi-objective particle swarm optimization algorithms: a study of many-objective problems. Neurocomputing **75**(1), 43–51 (2012)

Castillo-Villar, K.K., Smith, N.R., Herbert-Acero, J.F.: Design and optimization of capacitated supply chain networks including quality measures. Math. Probl. Eng., Article ID 218913, pp. 17 (2014)

Castillo-Villar, K.K., Smith, N.R., Simonton, J.L.: The impact of the cost of quality on serial supply-chain network design. Int. J. Prod. Res. **50**(19), 5544–5566 (2012)

Cerman, O., Husek, P.: Adaptive fuzzy sliding mode control for electro-hydraulic servo mechanism. Expert Syst. Appl. **39**(11), 10269–10277 (2012)

Cha, Y.S., Kim, K.G., Lee, J.Y., Lee, J., Choi, M., Jeong, M.H., Kim, C.H., You, B.J., Oh, S.R.: MAHRU-M: a mobile humanoid robot platform based on a dual-network control system and coordinated task execution. Robot. Auton. Syst. **59**(6), 354–366 (2011)

Chang, Y.H., Chang, C.W., Tao, C.W., Lin, H.W., Taur, J.S.: Fuzzy sliding-mode control for ball and beam system with fuzzy ant colony optimizationhttp://www.sciencedirect.com/science/article/pii/S0957417411013613. Expert Syst. Appl. vol. 39(3), 3624–3633 (2012)

Chen, Z., Meng, W., Zhang, J., Zeng, J.: Scheme of sliding mode control based on modified particle swarm optimization. Syst. Eng.Theory Pract. **29**(5), 137–141 (2009)

Dehghani, R., Fattah, A., Abedi, E.: Cyclic gait planning and control of a five-link biped robot with four actuators during single support and double support phases. Multibody Syst. dyn. (2013). doi:10.1007/s11044-013-9404-5

Ding, C.-T., Yang, S.-X., Gan, C.-B.: Input torque sensitivity to uncertain parameters in biped robot. Acta. Mech. Sin. **29**(3), 452–461 (2013)

Eberhart, R., Simpson, P., Dobbins, R.: Computational Intelligence PC Tools. Academic Press Professional, Inc, San Diego (1996)

Eberhart, R.C., Shi, Y.: Comparison between genetic algorithms and particle swarm optimization. Evolutionary Programming VII, pp. 611–616. Springer, Berlin (1998)

Eker, I.: Second-order sliding mode control with PI sliding surface and experimental application to an electromechanical plant. Arab. J. Sci. Eng. **37**(7), 1969–1986 (2012)

Elshazly, H.I., Azar, A.T., Elkorany, A.M., Hassanien, A.E.: Hybrid system based on rough sets and genetic algorithms for medical data classifications. Int. J. Fuzzy Syst. Appl. **3**(4), 31–46 (2013)

Engelbrecht, A.P.: Computational Intelligence: An Introduction. Wiley, New York (2002)

Engelbrecht, A.P.: Fundamentals of Computational Swarm Intelligence. Wiley, New York (2005)

Feng, S., Yahmadi Amur, S.A., Sun, Z.Q.: Biped walking on level ground with torso using only one actuator. Sci. China Inf. Sci. **56**(11), 1–9 (2013)

Fieldsend, J.E., Singh, S.: A multi-objective algorithm based upon particle swarm optimization and efficient data structure and turbulence, In: Workshop on Computational Intelligence, 2002, pp. 37–44

Fleming, P., Purshouse, R.: Evolutionary algorithms in control systems engineering: a survey. Control Eng. Pract. **10**(11), 1223–1241 (2002)

Fonseca, C., Fleming, P.: Multi-objective optimal controller design with genetic algorithms. Proceedings of the International Conference on Control, Coventry, 21–24 (1994) pp. 745–749 doi:10.1049/cp:19940225

Gaing, Z.L.: A particle swarm optimization approach for optimum design of PID controller in AVR system. IEEE Trans. Energy Convers. **19**(2), 384–391 (2004)

Gang, M., Wei, Z., Xiaolin, C.: A novel particle swarm optimization algorithm based on particle migration. Appl. Math. Comput. **218**(11), 6620–6626 (2012)

Gosh, A., Das, S., Chowdhury, A., Giri, R.: An ecologically inspired direct search method for solving optimal control problems with Bezier parameterization. Eng. Appl. Artif. Intell. **24**(7), 1195–1203 (2011)

Han, C., Zhang, G., Wu, L., Zeng, Q.: Sliding mode control of T-S fuzzy descriptor systems with time-delay. J. Franklin Inst. **349**(4), 1430–1444 (2012)

Hart, C.G., Vlahopoulos, N.: An integrated multidisciplinary particle swarm optimization approach to conceptual ship design. Struct. Multi. Optim. **41**(3), 481–494 (2010)

Hu, X., Eberhart, R.: Multi-objective optimization using dynamic neighborhood particle swarm optimization. In: Proceedings of the 2002 Congress on Evolutionary Computation, Honolulu, 2002, pp. 1677–1681. doi:10.1109/CEC.2002.1004494

Hu, J., Wang, Z., Gao, H., Stergioulas, L.K.: Robust H_∞ sliding mode control for discrete time-delay systems with stochastic nonlinearities. J. Franklin Inst. **349**(4), 1459–1479 (2012)

Islam, S., Liu, X.P.: Robust sliding mode control for robot manipulators. IEEE Trans. Industr. Electron. **58**(6), 2444–2453 (2011)

Jadhav, A.M., Vadirajacharya, K.: Performance verification of PID controller in an interconnected power system using particle swarm optimization. Energy Procedia **14**, 2075–2080 (2012)

Javadi-Moghaddam, J., Bagheri, A.: An adaptive neuro-fuzzy sliding mode based genetic algorithm control system for under water remotely operated vehicle. Expert Syst. Appl. **37**(1), 647–660 (2010)

Jia, D., Zheng, G., Qu, B., Khurram Khan, M.: A hybrid particle swarm optimization algorithm for high-dimensional problems. Comput. Ind. Eng. **61**(4), 1117–1122 (2011)

Jing, J., Wuan, Q.H.: Intelligent sliding mode control algorithm for position tracking servo system. Int. J. Inf. Technol. **12**(7), 57–62 (2006)

Kennedy, J., Eberhart, R.: Particle swarm optimization. In: Proceedings of IEEE International Conference on Neural Networks, Perth, 27 Nov–01 Dec 1995, pp. 1942–1948. doi:10.1109/ICNN.1995.488968

Ker-Wei, Y., Shang-Chang, H.: An application of AC servo motor using particle swarm optimization based sliding mode controller. Proceedings of IEEE International Conference on Systems, Man and Cybernetics, Taipei **8–11**, 4146–4150 (2006). doi:10.1109/ICSMC.2006.384784

Kim, B.-I., Son, S.-J.: A probability matrix based particle swarm optimization for the capacitated vehicle routing problem. J. Intell. Manuf. **23**(4), 1119–1126 (2012)

Kuo, R.J., Syu, Y.J., Chen, Z.-Y., Tien, F.C.: Integration of particle swarm optimization and genetic algorithm for dynamic clustering. Inf. Sci. **195**, 124–140 (2012)

Lari, A., Khosravi, A., Rajabi, F.: Controller design based on μ analysis and PSO algorithm. ISA Trans. **53**(2), 517–523 (2014)

Lee, J.H., Okamoto, S., Koike, H., Tani, K.: Development and motion control of a biped walking robot based on passive walking theory. Artif. Life Rob. **19**(1), 68–75 (2014)

Li, J., Li, W., Li, Q.: Sliding mode control for uncertain chaotic systems with input nonlinearity. Commun. Nonlinear Sci. Simul. **17**(1), 341–348 (2012)

Lin, C., Chen, L., Chen, C.: RCMAC hybrid control for MIMO uncertain nonlinear systems using sliding-mode technology. IEEE Trans. Neural Netw. **18**(3), 708–720 (2007)

Lin, T.C., Lee, T.Y., Balas, V.E.: Adaptive fuzzy sliding mode control for synchronization of uncertain fractional order chaotic systems. Chaos, Solitons Fractals **44**(10), 791–801 (2011)

Lin, C.J., Lin, P.T.: Particle swarm optimization based feedforward controller for a XY PZT positioning stage. Mechatronics **22**(5), 614–628 (2012)

Liu, C.-S., et al.: A new sliding control strategy for nonlinear system solved by the Lie-group differential algebraic equation method. Commun. Nonlinear Sci. Numer. Simul. **19**(6), 2012–2038 (2014)

Lu, C.H., Hwang, Y.R., Shen, Y.T.: Backstepping sliding mode tracking control of a vane-type air motor X-Y table motion system. ISA Trans. **50**(2), 278–286 (2011)

Mahmoodabadi, M.J., Arabani Mostaghim, S., Bagheri, A., Nariman-zadeh, N.:http://www.sciencedirect.com/science/article/pii/S0895717712001641 Pareto optimal design of the decoupled sliding mode controller for an inverted pendulum system and its stability simulation via Java programming. Math. Comput. Model. 57(5–6), 1070–1082 (2013)

Mahmoodabadi, M.J., Bagheri, A., Nariman-zadeh, N., Jamali, A., Abedzadeh Maafi, R.: Pareto design of decoupled sliding-mode controllers for nonlinear systems based on a multiobjective genetic algorithm. J. Appl. Math. Article ID 639014, pp. 22 (2012b)

Mahmoodabadi, M.J., Taherkhorsandi, M., Bagheri, A.: Pareto design of state feedback tracking control of a biped robot via multi-objective PSO in comparison with sigma method and genetic algorithms: modified NSGAII and MATLAB's toolbox. Sci. World J. 2014, p. 8 (2014b)

Mahmoodabadi, M.J., Bagheri, A., Arabani-Mostaghim, S., Bisheban, M.: Simulation of stability using Java application for Pareto design of controllers based on a new multi-objective particle swarm optimization. Math. Comput. Model. **54**(5–6), 1584–1607 (2011)

Mahmoodabadi, M.J., Bagheri, A., Nariman-zadeh, N., Jamali, A.: A new optimization algorithm based on a combination of particle swarm optimization, convergence and divergence operators for single-objective and multi-objective problems. Eng. Optim. **44**(10), 1167–1186 (2012a)

Mahmoodabadi, M.J., Taherkhorsandi, M., Bagheri, A.: Optimal robust sliding mode tracking control of a biped robot based on ingenious multi-objective PSO. Neurocomputing **124**, 194–209 (2014a)

Mahmoodabadi, M.J., Momennejad, S., Bagheri, A.: Online optimal decoupled sliding mode control based on moving least squares and particle swarm optimization. Inf. Sci. **268**, 342–356 (2014c)

Martínez-Soto, R., Castillo, O., Aguilar, L.T., Rodriguez, A.: A hybrid optimization method with PSO and GA to automatically design type-1 and type-2 fuzzy logic controllers. Int. J. Mach. Learn. Cybern. (2013). doi:10.1007/s13042-013-0170-8

Mondal, S., Mahanta, C.: Chattering free adaptive multivariable sliding mode controller for systems with matched and mismatched uncertainty. ISA Trans. **52**(3), 335–341 (2013a)

Mondal, S., Mahanta, C.: Adaptive integral higher order sliding mode controller for uncertain systems. J. Control Theory Appl. **11**(1), 61–68 (2013b)
Moosavian, S.A.A., Alghooneh, M., Takhmar, A.: Stable trajectory planning, dynamics modeling and fuzzy regulated sliding mode control of a biped robot. In: Proceedings of 7th IEEE-RAS International Conference on Humanoid Robots, Pittsburgh, Nov. 29–Dec. 1 2007, pp. 471–476. doi:10.1109/ICHR.2007.4813912
Mostaghim, S., Teich, J.: Strategies for finding good local guides in multi- objective particle swarm optimization (MOPSO). In: Proceedings of the 2003 IEEE Swarm Intelligence Symposium, 24–26 April 2003, pp. 26–33. doi:10.1109/SIS.2003.1202243
Mousa, A.A., El-Shorbagy, M.A., Abd-El-Wahed, W.F.: Local search based hybrid particle swarm optimization algorithm for multi objective optimization. Swarm Evol. Comput. **3**, 1–14 (2012)
Nejat, A., Mirzabeygi, P., Shariat Panahi, M.: Airfoil shape optimization using improved multiobjective territorial particle swarm algorithm with the objective of improving stall characteristics. Struct. Multi. Optim. **49**(6), 953–967 (2014)
Nery Júnior, G.A., Martins, M.A.F., Kalid, R.: A PSO-based optimal tuning strategy for constrained multivariable predictive controllers with model uncertainty. ISA Trans. **53**(2), 560–567 (2014)
Nikkhah, M., Ashrafiuon, H., Fahimi, F.: Robust control of under actuated bipeds using sliding modes. Robatica **25**(3), 367–374 (2007)
Nizar, A., Mansour Houda, B., Ahmed Said, N.: A new sliding function for discrete predictive sliding mode control of time delay systems. Int. J. Autom. Comput. **10**(4), 288–295 (2013)
Nwankwor, E., Nagar, A.K., Reid, D.C.: Hybrid differential evolution and particle swarm optimization for optimal well placement. Comput. Geosci. **17**(2), 249–268 (2013)
Pan, I., Korre, A., Das, S., Durucan, S.: Chaos suppression in a fractional order financial system using intelligent regrouping PSO based fractional fuzzy control policy in the presence of fractional Gaussian noise. Nonlinear Dyn. **70**(4), 2445–2461 (2012)
Parsopoulos, K.E., Tasoulis, D.K., Vrahatis, M.N.: Multi-objective optimization using parallel vector evaluated particle swarm optimization. Proceedings of the IASTED International Conference on Artificial Intelligence and Applications. vol. 2, 823–828 (2004)
Pourmahmood Aghababa, M., Akbari, M.E.: A chattering-free robust adaptive sliding mode controller for synchronization of two different chaotic systems with unknown uncertainties and external disturbances. Appl. Math. Comput. **218**(9), 5757–5768 (2012)
Qiao, W., Venayagamoorthy, G., Harley, R.: Design of optimal PI controllers for doubly fed induction generators driven by wind turbines using particle swarm optimization. In: Proceedings of the International Joint Conference on Neural Networks, Vancouver, 2006, pp. 1982–1987. doi:10.1109/IJCNN.2006.246944
Ramos, R., Biel, D., Fossas, E., Griño, R.: Sliding mode controlled multiphase buck converter with interleaving and current equalization. Control Eng. Pract. **21**(5), 737–746 (2013)
Ratnaweera, A., Halgamuge, S.K.: Self-organizing hierarchical particle swarm optimizer with time-varying acceleration coefficient. IEEE Trans. Evol. Comput. **8**(3), 240–255 (2004)
Sanchez, G., Villasana, M., Strefezza, M.: Multi-objective pole placement with evolutionary algorithms. Lect. Notes Comput. Sci. **4403**, 417–427 (2007)
Shahriari kahkeshi, M., Sheikholeslam, F., Zekri, M.: Design of adaptive fuzzy wavelet neural sliding mode controller for uncertain nonlinear systems. ISA Trans. **52**(3), 342–350 (2013)
Singla, M., Shieh, L.-S., Song, G., Xie, L., Zhang, Y.: A new optimal sliding mode controller design using scalar sign function. ISA Trans. **53**(2), 267–279 (2014)
Sira-Ramirez, H., Luviano-Juarez, A., Cortes-Romero, J.: Robust input-output sliding mode control of the buck converter. Control Eng. Pract. **21**(5), 671–678 (2013)
Sun, T., Pei, H., Pan, Y., Zhou, H., Zhang, C.: Neural network-based sliding mode adaptive control for robot manipulators. Neurocomputing **74**(14–15), 2377–2384 (2011)
Tang, Y., Wang, Z., Fang, J.: Controller design for synchronization of an array of delayed neural networks using a controllable probabilistic PSO. Inf. Sci. **181**(20), 4715–4732 (2011)
Toscana, R.: A simple robust PI/PID controller design via numerical optimization approach. J. Process Control **15**(1), 81–88 (2005)

Utkin, V.I.: Sliding Modes and their Application in Variable Structure Systems. Central Books Ltd, London (1978)

Wai, R.J., Chuang, K.L., Lee, J.D.: Total sliding-model-based particle swarm optimization controller design for linear induction motor, In: Proceedings of IEEE Congress on Evolutionary Computation, 25–28 Sept. 2007, Singapore. pp. 4729–4734

Wang, K., Jun Zheng, Y.: A new particle swarm optimization algorithm for fuzzy optimization of armored vehicle scheme design. Appl. Intell. **37**(4), 520–526 (2012)

Wang, X., Tang, L.: A discrete particle swarm optimization algorithm with self-adaptive diversity control for the permutation flowshop problem with blocking. Appl. Soft Comput. **12**(2), 652–662 (2012)

Winter, D.A.: Biomechanics and Motor Control of Human Movement. Wiley, New York (1990)

Wolovich, W.A.: Automatic Control Systems: Basic Analysis and Design. Saunders College Publishing, USA (1994)

Xiuping, M., Qiong, W.: Dynaimc modeling and sliding mode control of a five-link biped during the double support phase. In the Proceedings of the 2004 American Control Conference, vol. 3, pp. 2609-2614 (2004)

Yakut, O.: Application of intelligent sliding mode control with moving sliding surface for overhead cranes. Neural Comput. Appl. **24**(6), 1369–1379 (2014)

Yildiz, A.R., Solanki, K.N.: Multi-objective optimization of vehicle crashworthiness using a new particle swarm based approach. Int. J. Adv. Manuf. Technol. **59**(1–4), 367–376 (2012)

Yin, C., Zhong, S.M., Chen, W.F.: Design of sliding mode controller for a class of fractional-order chaotic systems. Commun. Nonlinear Sci. Simul. **17**(1), 356–366 (2012)

Yoshida, H., Kawata, K., Fukuyama, Y.: A particle swarm optimization for reactive power and voltage control considering voltage security assessment. IEEE Trans. Power Syst. **15**(4), 1232–1239 (2000)

Zhang, R., Sun, C., Zhang, J., Zhou, Y.: Second-order terminal sliding mode control for hypersonic vehicle in cruising flight with sliding mode disturbance observer. J. Control Theory Appl. **11**(2), 299–305 (2013)

Zhang, Y., Yao, F., Iu Ho-Ching, H., Fernando, T., Po Wong, K.: Sequential quadratic programming particle swarm optimization for wind power system operations considering emissions. J. Mod. Power Syst. Clean Energy **1**(3), 231–240 (2013)

Zheng, Z., Wu, C.: Power optimization of gas pipelines via an improved particle swarm optimization algorithm. Petrol. Sci. **9**(1), 89–92 (2012)

http://www.springer.com/978-3-319-11172-8

Advances and Applications in Sliding Mode Control systems

Azar, A.T.; Zhu, Q. (Eds.)
2015, XI, 590 p. 280 illus., Hardcover
ISBN: 978-3-319-11172-8